a

b

Figure 7 p73 and cisplatin treatment activate the expression of DNA repair genes. (a) Induction of the promoter activity by p73. Rad51 Luc or FEN-1 Luc was transiently co-transfected with p73 expression plasmid and CH110 plasmid (Amersham Biosciences, Piscataway, NJ, USA) expressing β-galactosidase as an internal control. The results are normalized to β-galactosidase activity and are representative of at least three independent experiments. Bars, $\pm$s.d. (b) Enhancement of DNA binding activity of ZNF143 by cisplatin treatment. Soluble chromatin was prepared from Flag-ZNF143 stable transfectant untreated (lanes 1, 3 and 5) or treated (lanes 2, 4 and 6) with cisplatin, and immunoprecipitated with anti-mouse IgG (lanes 3 and 4) or anti-Flag (M2) antibodies (lanes 5 and 6). Extracted DNAs of immunoprecipitation (lanes 3–6) and soluble chromatin (lanes 1 and 2) were amplified using specific primer pairs for the *Rad51* and *FEN-1* promoter regions. Amplification products were subjected by electrophoresis as described in Figure 6d.

number of DNA repair genes contain potential binding site for ZNF143 in their regulatory regions (Supplementary Data). These results suggest that ZNF143 is a positive regulator like a master gene for the expression of DNA repair genes.

In conclusion, our data indicate that ZNF143 is a pivotal transcription factor that regulates the gene expression for DNA repair pathways together with p73 and is involved in cisplatin resistance. Our findings also raise the possibility that inhibition of ZNF143 function might be a target for therapeutic augmentation of cisplatin-based chemotherapy. Further investigation to define the molecular function of ZNF143 will greatly advance our understanding of cisplatin resistance.

Materials and methods

Cell culture

Human epidermoid cancer KB cells and human prostate cancer PC3 cells were cultured in Eagle's minimal essential medium (Nissui Seiyaku, Tokyo, Japan) containing 10% heat-inactivated fetal bovine serum. The cisplatin-resistant KB/CP4 and P/CDP6 cells were derived from KB and PC3 as described previously (Tanabe *et al.*, 2003). Seven lung cancer cell lines

were obtained as described previously (Sugaya *et al.*, 2002). Cell lines were maintained in a 5% CO_2 atmosphere at 37°C.

Antibodies and drugs

Anti-Flag (M2) monoclonal antibody and anti-Flag (M2) affinity gel were purchased from Sigma (St Louis, MO, USA). Anti-STAT3 (sc-482), anti-proliferating cell nuclear antigen (PCNA) (sc-56) and HA-probe (F-7) AC (agarose conjugate) were purchased from Santa Cruz Biotechnology (Santa Cruz, CA, USA). Anti-Rad51, anti-FEN-1 antibodies and anti-HA-peroxidase (3F10) were purchased from Calbiochem (Darmstadt, Germany), BD Biosciences (BD Biosciences Clontech, Palo Alto, CA, USA) and Roche molecular Biochemicals (Mannheim, Germany), respectively. The anti-ZNF143 antibody was kindly gifted by Dr GR Kunkel (Texas A&M University, TX, USA) (Ishiguchi *et al.*, 2004). Cisplatin, vincristine and etoposide were purchased from Sigma. Oxaliplatin was kindly provided from Yakult Honsha Co., Ltd., Tokyo, Japan.

Plasmid construction

Plasmid construction of pGEX-p53, pGEX-p73 and pGEX-ZNF143 that express GST-p53, GST-p73 and GST-ZNF143 proteins in bacteria, respectively, and pcDNA3-HA-p53 that expresses HA-p53 protein in mammalian cells were described previously (Imamura *et al.*, 2001; Uramoto *et al.*, 2002, 2003). pcDNA3-HA-p73 expression plasmid in mammalian cells was kindly provided by Dr G Melino (University of Rome, Rome, Italy) (De Laurenzi *et al.*, 1998). For construction of pcDNA3-3 × Flag expression plasmid, the following double-stranded oligonucleotides were inserted to pcDNA3 expression plasmid (Invitrogen, San Diego, CA, USA) between *Bam*HI and *Eco*RI sites. Three times Flag oligonucleotides; 5'-ATGGACTACAAAGACCATGACGGTGATTATAAAGAT CATGACATCGATTACAAGGATGACGATGACAAGAAT TGG-3'. To obtain the pcDNA3-3 × Flag ZNF143, full length of ZNF143 cDNA was ligated at C-terminal of 3 × Flag in pcDNA3-3 × Flag mammalian expression plasmid. For construction of pIRES/hygro-3 × Flag ZNF143, *Bam*HI–*Not*I fragment containing 3 × Flag ZNF143 was obtained by digesting the pcDNA3-3 × Flag ZNF143 plasmid with *Bam*HI and *Not*I, and ligated in same sites of pIRES/hygro mammalian expression plasmid (BD Biosciences Clontech). To obtain Rad51 Luc and FEN-1 Luc, *Rad51* and *FEN-1* promoters were amplified by polymerase chain reaction (PCR) with the following primer pairs with restriction enzyme cleavage sites at the 5' end; 5'-AGATCTGCGATGGTGAGAACTCGCGGA CC-3' and 5'-AAGCTTCACCCCGCGGGCGTGGCACG-3' for the *Rad51* promoter (−471 to +211); 5'-AGATCTGTA-CAGAGGCTGTGGGCGCTCC-3' and 5'-AAGCTTGGTT CGGGGTTGCCCCGGGC-3' for the *FEN-1* promoter (−525 to +319). These PCR products were cloned into the pGEM-T easy vector (Promega, Madison, WI, USA). The promoter fragments were gel-purified after *Bgl*II–*Hin*dIII digestion and ligated into the *Bgl*II–*Hin*dIII site of pGL3-basic vector (Promega).

Cloning of stable transfectants

Two micrograms of pIRES/hygro vector or pIRES/hygro-3 × Flag ZNF143 was transfected into 1 × 10^5 cells of PC3 using 10 µl Superfect reagent (Qiagen, Hilden, Germany) according to the manufacturer's instructions. After 24 h of transfection, the cells were trypsinized and plated on 100-mm dishes with dilution to form colonies and cultured with maintenance medium containing 250 µg/ml hygromycin. The resulting colonies were isolated using cloning cylinders and transferred to 24-well plates. Cellular expression level of

3 × Flag ZNF143 in each clones was investigated by following Western blotting with anti-Flag antibody. Stable transfectant with expression of 3 × Flag ZNF143 was named PC3/3 × Flag ZNF143 (PC3/3FZ) and was used in this study. PC3/control vector (PC3/CV) was also selected by the transfection with pIRES/hygro vector alone.

Northern blotting
Northern blotting analysis was performed as described previously (Murakami *et al.*, 2001; Ishiguchi *et al.*, 2004). Briefly, total RNA was isolated using the Sepasol reagent (Nacalai Tesque, Kyoto, Japan). RNA samples (20 μg/lane) were separated on a 1% formaldehyde agarose gel and transferred to a hybond N+ membrane (GE Healthcare Bio-Science, Piscataway, NJ, USA) with 10 × SSC. ZNF143 cDNA fragments were labeled with random primers using the Megaprime DNA labeling kit (GE Healthcare Bio-Science). After prehybridization and hybridization, signal intensities were quantified using a bio-imaging analyzer (FLA2000, Fuji Photo Film, Tokyo, Japan).

Western blotting
Whole-cell lysates and eluted nuclear extracts were prepared as described previously (Uramoto *et al.*, 2002). To prepare whole-nuclear protein, isolated nuclei was directly sonicated for 10 s and designated as nuclear fractions. The indicated amounts of whole-cell lysates, nuclear extracts or nuclear fractions were separated by sodium dodecyl sulfate–polyacrylamide gel electrophoresis (SDS–PAGE). The proteins were transferred to a polyvinylidine difluoride microporous membranes (Millipore, Bedford, MA, USA) using a semi-dry blotter. The blotted membrane was treated with 5% (w/v) skimmed milk in 10 mM Tris, 150 mM NaCl, 0.2% (v/v) Tween 20 and incubated for 2 h at 4°C with a 1:5000 dilution of anti-ZNF143, a 1:10000 dilution of anti-Flag (M2), a 1:2000 dilution of anti-PCNA, a 1:1000 dilution of anti-STAT3, a 1:500 dilution of anti-FEN-1 and a 1:1000 dilution of anti-Rad51 antibodies. The membrane was then incubated for 40 min at room temperature with a peroxidase-conjugated secondary antibody or a 1:5000 dilution of anti-HA-peroxidase. It was treated with an ECL kit (GE Healthcare Bio-Science) and exposed to Kodak X-OMAT film by autoradiography. The intensity in each signal was assessed numerically by NIH image program (NIH, Bethesda. MD, USA).

Transient transfections and co-immunoprecipitation assay
Transient transfection and immunoprecipitation assay were performed as described previously (Uramoto *et al.*, 2002; Izumi *et al.*, 2003). Briefly, 1 × 10⁵ PC3 cells were seeded into six-well tissue-culture plates. The following day, both 1 μg HA and 3 × Flag expression plasmids were transfected using Superfect reagent (Qiagen) according to the manufacturer's instructions. Three hours post-transfection, the cells were washed with phosphate-buffered saline, cultured at 37°C for 48 h in fresh medium and then lysed in buffer X containing 50 mM Tris-HCl (pH 8.0), 1 mM ethylenediaminetetraacetic acid (EDTA), 120 mM NaCl, 0.5% Nonidet P-40, 10% glycerol, 1 mM phenylmethylsulfonyl fluoride and 1 μM ZnCl₂. After incubating for 30 min on ice, the lysates were centrifuged at 21 000 g for 10 min at 4°C. The supernatant (300 μg) was incubated for 2 h at 4°C with anti-Flag M2 affinity gel or HA-probe (F-7) AC, and the beads were washed three times with buffer X. Immunoprecipitated samples and pre-immunoprecipitated samples (50 μg) were separated by SDS–PAGE, and Western blotting analysis was performed with anti-Flag antibody and anti-HA-peroxidase as described above.

Knockdown analysis using siRNAs
Three kinds of double-stranded ZNF143 RNA 25 bp oligonucleotides were generated from Stealth Select RNAi (Invitrogen) No. 1. 5'-UAACCAUAGCAACAGAGUGCGUUCC-3' and 5'-GGAACGCACUCUGUUGCUAUGGUUA-3'; No. 2. 5'-UAAUUUGUUGCACUGGCAAAUGCCC-3' and 5'-GGGCAUUUGCCAGUGCAACAAAUUA-3'; and No. 3. 5'-AUAAGCUGUGGUACCAUCUUCCAGC-3' and 5'-GC UGGAAGAUGGUACCACAGCUUAU-3'. siRNA transfections were performed according to the manufacturer's instructions (Invitrogen). Briefly, 1 μl lipofectamine transfection reagent (Invitrogen) was diluted in 250 μl Opti-minimum essential medium (MEM) I medium (Invitrogen) and incubated for 5 min at room temperature. Next, 50 or 100 pmol ZNF143 siRNA and Stealth RNAi negative control with medium GC (Invitrogen) diluted in 250 μl Opti-MEM I were added gently and incubated for 20 min at room temperature. Oligomer–Lipofectamine complexes and aliquots of 2 × 10⁵ PC3 or P/CDP6 cells in 2 ml culture medium were combined and incubated for 10 min at room temperature. Aliquots of 4 × 10² PC3 cells or 6 × 10² P/CDP6 cells were used for a colony-formation assay as described below. The remaining cells were seeded in 35 mm dishes with 2 ml culture medium and harvested after 72 h culture for Western blotting analysis as described above.

Cytotoxicity assay
For the colony-formation assay, 4 × 10² PC3 or 6 × 10² P/CDP6 cells transfected with siRNAs were seeded in 35 mm dishes with 2 ml culture medium. The following day, the cells were treated with indicated concentrations of cisplatin, oxaliplatin, etoposide and vincristine. After 7 days, the number of colonies was counted.

Purification of GST fusion protein
Induction and purification of GST fusion proteins were described previously (Ise *et al.*, 1999). Briefly, *Escherichia coli* cells transformed with GST expression plasmids were induced by isopropyl-1-thio-γ-D-galactopyranoside for 1 h and sonicated for 10 s in buffer X as described above. Soluble fractions were obtained by centrifugation at 21 000 g for 10 min at 4°C. GST fusion proteins were bound to 10 μl glutathione-sepharose 4B in a 50% slurry in buffer X for 4 h at 4°C, washed three times with buffer X and eluted with 50 mM Tris-HCl (pH 8.0) and 20 mM reduced glutathione according to the manufacturer's protocol (GE Healthcare Bio-Science).

Electrophoretic mobility shift assay
The sequences of the oligonucleotides used for the probes in EMSAs were as follows: human *U6 RNA* oligo, 5'-GCC TATTTCCCATGATTCCTTCATATTTGC-3' and 5'-GGGC AAATATGAAGGAATCATGGGAAATAGG-3'; human *Rad51* oligo, 5'-GGTACATCTCCCGGCATGCATCGCCG GCG-3' and 5'-GGCGCCGGCGATGCATGCCGGGAGAT GTA-3'; human *FEN-1* oligo, 5'-GGACCCGTGCCCATCC TACAATGCCCTGG-3' and 5'-GGCCAGGGCATTGTAG GATGGGCACGGGT-3'; GC oligo for modification of cisplatin, 5'-GGCCGGGGCGGGGCGATCGGGGCGGGGGC-3' and 5'-GGGCCCCCGCCCCGATCGCCCCGCCCCGG. The ZNF143 binding sites in these oligonucleotide probes were underlined (see Figure 6a). Preparation of the ³²P-labeled oligonucleotide probes were described previously (Imamura *et al.*, 2001; Ishiguchi *et al.*, 2004). Briefly, the oligonucleotides were annealed with complementary strands. The double-stranded products were end-labeled with [α-³²P] deoxycytidimine triphosphate (GE Healthcare Bio-Science) using the

Klenow fragment (Fermentas, Vilnius, Lithuania) and purified from gel. For preparation of cispaltin-modified DNA, labeled GC oligonucleotide probe was treated with 0.3 mM cisplatin at 37°C for 6 h and purified by ethanol precipitation. EMSAs with purified GST fusion proteins were performed as described previously (Imamura et al., 2001; Ishiguchi et al., 2004). Briefly, GST fusion proteins were incubated for 5 min at room temperature in a final volume of 20 μl containing 10 mM Tris-HCl (pH 7.5), 50 mM NaCl, 5 mM MgCl$_2$, 10 μM ZnCl$_2$, 1 mM EDTA, 1 mM dithiothreitol, 0.1 mg/ml bovine serum albumin, 10% glycerol, 0.05% Nonidet P-40 and 4 ng ^{32}P-oligonucleotide probe. The reaction mixtures were resolved by electrophoresis on a 4% polyacrylamide gel (polyacrylamide/bisacrylamide, 80:1) by 10 V/cm for 90–120 min at room temperature with 0.5 × tris-borate-EDTA (TBE) buffer (45 mM Tris base, 45 mM boric acid and 1 mM EDTA). The gel was dried and analysed by a bio-imaging analyzer (FLA2000).

ChIP assay

The ChIP assay was performed as described previously (Uramoto et al., 2002). Both PC3/CV and PC3/3FZ stable transfectants were treated with or without 20 μM cisplatin for 12 h. Briefly, protein–DNA crosslinking was performed by incubating PC3/control vector and PC3/3 × Flag-ZNF143 cells with formaldehyde. The cells were lysed in radioimmunoprecipitation assay buffer (50 mM Tris-HCl (pH 7.5), 1 mM EDTA, 150 mM NaCl, 0.1% SDS, 0.5% sodium deoxycholate, 1% Nonidet P-40 and 1 mM phenylmethylsulfonyl fluoride) and the lysates were sonicated. Soluble chromatin from 1 × 10^6 cells was incubated with 5 μg/ml anti-Flag (M2) affinity gel or anti-mouse immunoglobulin G (IgG) with protein A/G agarose (Santa Cruz) by rotation for 2 h at 4°C. Immune complexes were collected by centrifugation. They were then treated with 0.2 M NaCl to reverse protein–DNA crosslinking, and were digested with proteinase K and RNase A. The purified DNA was dissolved with 20 μl dH$_2$O. The DNA (1 μl) was then used for PCR analysis with the following primer pairs for the Rad51 promoter region (−471 to +211): 5′-AGATCTGCGATGGTGAGAACTCGCGGACC-3′ forward primer and 5′-AAGCTTCACCCCGCGGGCGTGGCACG-3′ reverse primer; for the FEN-1 promoter region (−525 to +319): 5′-AGATCTGTACAGAGGCTGTGGGCGCTCC-3′ forward primer and 5′-AAGCTTGGTTCGGGGTTGCCCCGGGC-3′ reverse primer; the PRDX4 promoter region (−121 to +36): 5′-AGATCTGCCCACGTGGCGGGGCGGGGAGC-3′ for-

ward primer and 5′-CTCGAGCGCAGAAACACGTCCCTT GGCG-3′ reverse primer. The PCR products were separated by electrophoresis on a 2% agarose gel and stained with ethidium bromide.

Transient transfection and luciferase assay

Transient transfection and a luciferase assay were performed as described previously (Uramoto et al., 2002). Briefly, 5 × 10^4 PC3 cells were seeded into 12-well tissue-culture plates. The following day, 0.2 μg of Rad51 or FEN-1 reporter plasmid was transfected with 1.2 μg of p73 expression plasmid using 3 μl/well Superfect reagent (Qiagen) according to the manufacturer's instructions. Three hours post-transfection, the cells were washed and cultured at 37°C for 48 h in fresh medium. Luciferase activity using cell lysated with lysis buffer and brief centrifugation was detected by a Picagene kit (Toyoinki, Tokyo, Japan), and the light intensity was measured with a luminometer (Luminescencer JNII RAB-2300; ATTO, Japan) according to the manufacturer's instructions.

ZNF143 binding site analysis

The search for ZNF143 binding site was performed using the DataBase of Transcriptional Start Sites software version 5.2. 0 (http://dbtss.hgc.jp) developed by Dr Sumio Sugano and Dr Yutaka Suzuki and the Searching Transcription Factor Binding Sites software version 1.3 (http://mbs.cbrc.jp/research/db/TFSEARCH.html) developed by Dr Yutaka Akiyama. Briefly, each 1000 bp upstream region from transcriptional Start Site was obtained by the DataBase of Transcriptional start sites software with GeneID number of Entrez Gene database in National Center for Biotechnology Information. Then, staf binding site (19 bp consensus sequence), which is the same as ZNF143 binding site, was searched by the Searching Transcription Factor Binding Sites software with 70 threshold score. More than 150 genes associated with DNA repair were searched, and 83 ZNF143 binding sites in the 62 genes were found. These results were listed in a Supplementary Data.

References

Altaha R, Liang X, Yu JJ, Reed E. (2004). Excision repair cross complementing-group 1: gene expression and platinum resistance. Int J Mol Med 14: 959–970.

Bhattacharyya A, Ear US, Koller BH, Weichselbaum RR, Bishop DK. (2000). The breast cancer susceptibility gene BRCA1 is required for subnuclear assembly of Rad51 and survival following treatment with the DNA cross-linking agent cisplatin. J Biol Chem 275: 23899–23903.

Chaney SG, Sancar A. (1996). DNA repair: enzymatic mechanisms and relevance to drug response. J Natl Cancer Inst 88: 1346–1360.

Cohen SM, Lippard SJ. (2001). Cisplatin: from DNA damage to cancer chemotherapy. Prog Nucleic Acid Res Mol Biol 67: 93–130.

De Laurenzi V, Costanzo A, Barcaroli D, Terrinoni A, Falco M, Annicchiarico-Petruzzelli M et al. (1998). Two new p73 splice

variants, γ and δ, with different transcriptional activity. J Exp Med 188: 1763–1768.

Fujii R, Mutoh M, Niwa K, Yamada K, Aikou T, Nakagawa M et al. (1994). Active efflux system for cisplatin in cisplatin-resistant human KB cells. Jpn J Cancer Res 85: 426–433.

Imamura T, Izumi H, Nagatani G, Ise T, Minoru N, Iwamoto Y et al. (2001). Interaction with p53 enhances binding of cisplatin-modified DNA by high mobility group 1 protein. J Biol Chem 276: 7534–7540.

Ise T, Nagatani G, Imamura T, Kato K, Takano H, Nomoto M et al. (1999). Transcription factor Y-Box binding protein 1 binds preferentially to cisplatin-modified DNA and interacts with proliferating cell nuclear antigen. Cancer Res 59: 342–346.

Ishiguchi H, Izumi H, Torigoe T, Yoshida Y, Kubota H, Tsuji S et al. (2004). ZNF143 activates gene expression in

response to DNA damage and binds to cisplatin-modified DNA. *Int J Cancer* **111**: 900–909.

Izumi H, Ohta R, Nagatani G, Ise T, Nakayama Y, Nomoto M *et al.* (2003). p300/CBP-associated factor (P/CAF) interacts with nuclear respiratory factor-1 to regulate the UDP-N-acetyl-alpha-D-galactosamine: polypeptide *N*-acetylgalacto-saminyltransferase-3 gene. *Biochem J* **373**: 713–722.

Keshelava N, Zuo JJ, Chen P, Waidyaratne SN, Luna MC, Gomer CJ *et al.* (2001). Loss of p53 function confers high-level multidrug resistance in neuroblastoma cell lines. *Cancer Res* **61**: 6185–6193.

Kohno K, Izumi H, Uchiumi T, Ashizuka T, Kuwano M. (2003). The pleiotropic functions of the Y-box-binding protein, YB-1. *Bioessays* **25**: 691–698.

Kohno K, Uchiumi T, Niina I, Wakasugi T, Igarashi T, Momii Y *et al.* (2005). Transcription factors and drug resistance. *Eur J Cancer* **41**: 2577–2586.

Kuwano M, Oda Y, Izumi H, Yang SJ, Uchiumi T, Iwamoto Y *et al.* (2004). The role of nuclear Y-box binding protein 1 as a global marker in drug resistance. *Mol Cancer Ther* **3**: 1485–1492.

Lieber MR. (1997). The FEN-1 family of structure-specific nucleases in eukaryotic DNA replication, recombination and repair. *Bioessays* **19**: 233–240.

Murakami T, Shibuya I, Ise T, Chen AS, Akiyama S, Nakagawa M *et al.* (2001). Elevated expression of vacuolar proton pump genes and cellular pH in cisplatin resistance. *Int J Cancer* **93**: 869–874.

Myslinski E, Krol A, Carbon P. (1998). ZNF76 and ZNF143 are two human homologs of the transcriptional activator staf. *J Biol Chem* **34**: 21998–22006.

Ohga T, Koike K, Ono M, Makino Y, Itagaki Y, Tanimoto M *et al.* (1996). Role of the human Y box-binding protein YB-1 in cellular sensitivity to the DNA-damaging agents cisplatin, mitomycin C, and ultraviolet light. *Cancer Res* **56**: 4224–4228.

Raymond E, Faivre S, Chaney S, Woynarowski J, Cvitkovic E. (2002). Cellular and molecular pharmacology of oxaliplatin. *Mol Cancer Ther* **1**: 227–235.

Rincon JC, Engler SK, Hargrove BW, Kunkel GR. (1998). Molecular cloning of a cDNA encoding human SPH-

binding factor, a conserved protein that binds to the enhancer-like region of the U6 small nuclear RNA gene promoter. *Nucleic Acids Res* **26**: 4846–4852.

Schaub M, Myslinski E, Schuster C, Krol A, Carbon P. (1997). Staf, a promiscuous activator for enhanced transcription by RNA polymerase II and III. *EMBO J* **16**: 173–181.

Spiro C, McMurray CT. (2003). Nuclease-deficient FEN-1 blocks Rad51/BRCA1-mediated repair and causes trinucleo-tide repeat instability. *Mol Cell Biol* **23**: 6063–6074.

Sugaya M, Takenoyama M, Osaki T, Yasuda M, Nagashima A, Sugio K *et al.* (2002). Establishment of 15 cancer cell lines from patients with lung cancer and the potential tools for immunotherapy. *Chest* **122**: 282–288.

Tanabe M, Izumi H, Ise T, Higuchi S, Yamori T, Yasumoto K *et al.* (2003). Activating transcription factor 4 increases the cisplatin resistance of human cancer cell lines. *Cancer Res* **63**: 8592–8595.

Tew KD. (1994). Glutathione-associated enzymes in antic-ancer drug resistance. *Cancer Res* **54**: 4313–4320.

Torigoe T, Izumi H, Ishiguchi H, Yoichiro Y, Mizuho T, Takeshi Y *et al.* (2005). Cisplatin resistance and transcrip-tion factors. *Curr Med Chem Anticancer Agents* **5**: 15–27.

Uramoto H, Izumi H, Ise T, Tada M, Uchiumi T, Kuwano M *et al.* (2002). p73 interacts with c-Myc to regulate Y-box-binding protein-1 expression. *J Biol Chem* **277**: 31694–31702.

Uramoto H, Izumi H, Nagatani G, Ohmori H, Nahasue N, Ise T *et al.* (2003). Physical interaction of tumour suppressor p53/p73 with CCAAT-binding transcription factor 2 (CTF2) and differential regulation of human high-mobility group 1 (HMG1) gene expression. *Biochem J* **371**: 301–310.

Vikhanskaya F, Marchini S, Marabese M, Galliera E, Broggini M. (2001). p73α overexpression is associated with resistance to treatment with DNA-damaging agents in a human ovarian cancer cell line. *Cancer Res* **61**: 935–938.

Wood RD, Mitchell M, Lindahl T. (2005). Human DNA repair genes, 2005. *Mut Res* **577**: 275–283.

Zamble DB, Lippard SJ. (1995). Cisplatin and DNA repair in cancer chemotherapy. *Trends Biochem Sci* **20**: 435–439.

Supplementary Information accompanies the paper on the Oncogene website (http://www.nature.com/onc).

Antibody-dependent cellular cytotoxicity of cetuximab against tumor cells with wild-type or mutant epidermal growth factor receptor

Hideharu Kimura,[1,2] Kazuko Sakai,[1] Tokuzo Arao,[1,3] Tatsu Shimoyama[1,4] Tomohide Tamura[5] and Kazuto Nishio[1,3,6]

[1]Shien-Laboratory, National Cancer Center Hospital, Tsukiji 5-1-1, Chuo-ku, Tokyo 104-0045; [2]Respiratory Medicine, Kanazawa University Hospital, Takara-machi 13-1, Kanazawa, Ishikawa, 920-8641; [3]Department of Genome Biology, Kinki University School of Medicine, 377-2 Ohno-Higashi Osaka-Sayama, Osaka, 589-8511; [4]Department of Chemotherapy, Tokyo Metropolitan Komagome Hospital, 3-18-22 Honkomagome, Bunkyo-ku, Tokyo, 113-8677; [5]Medical Oncology, National Cancer Center Hospital, Tsukiji 5-1-1, Chuo-ku, Tokyo 104-0045, Japan

Cetuximab (Erbitux, IMC-C225) is a monoclonal antibody targeted to the epidermal growth factor receptor (EGFR). To clarify the mode of antitumor action of cetuximab, we examined antibody-dependent cellular cytotoxicity (ADCC) activity against several tumor cell lines expressing wild-type or mutant EGFR. ADCC activity and complement-dependent cytolysis activity were analyzed using the CytoTox 96 assay. ADCC activities correlated with the EGFR expression value ($R = 0.924$). ADCC activities were detected against all tumor cell lines, except K562 cells in a manner dependent on the cellular EGFR expression level, whereas complement-dependent cytolysis activity was not detected in any of the cell lines. The ADCC activity mediated by cetuximab was examined in HEK293 cells transfected with wild-type EGFR (293W) and a deletional mutant of EGFR (293D) in comparison with the mock transfectant (293M). ADCC activity was detected in 293W and 293D cells, in a cetuximab dose-dependent manner, but not in 293M cells (<10%). These results indicate that ADCC-dependent antitumor activity results from the degree of affinity of cetuximab for the extracellular domain of EGFR, independent of EGFR mutation status. These results suggest ADCC activity to be one of the modes of therapeutic action of cetuximab and to depend on EGFR expression on the tumor cell surface. (*Cancer Sci* 2007; 98: 1275–1280)

The epidermal growth factor receptor (EGFR) is a member of the ErbB family of receptors that is abnormally activated in many malignancies. EGFR is frequently overexpressed or abnormally activated in tumors. EGFR overexpression correlates with a worse outcome.[1,2] Early studies with anti-EGFR monoclonal antibodies (mAb) were shown to inhibit the growth of cancer cells bearing EGFR.[3]

Cetuximab (IMC-225, Erbitux) is a recombinant, human–murine chimeric mAb that is produced in mammalian (murine myeloma) cell culture and targeted specifically to EGFR. Cetuximab is composed of a murine Fv (EGFR-binding) lesion and a human IgG1 heavy and κ light chain Fc (constant) region. *In vitro* studies have shown that cetuximab competes with endogenous ligands to bind with the external domain of EGFR. Cetuximab binds to EGFR with 10-fold higher affinity than endogenous ligands (0.1–0.2 nM cetuximab *vs* 1 nM epidermal growth factor [EGF] or transforming growth factor (TGF)-α, respectively).[4] Cetuximab has shown promising preclinical and clinical activity in a variety of tumor types.[5]

The anti-tumor strategy is to direct mAb to the ligand-binding extracellular domain and to prevent ligand binding and ligand-dependent receptor inhibition. The use of humanized murine–human chimeric mAb of the IgG1 subtype is now well established for the treatment of human cancers. Treatment of advanced breast cancer with human epidermal growth factor receptor type 2 (HER-2)-specific trastuzumab (Herceptin) and of follicular non-Hodgkin B-cell lymphoma with CD20-specific rituximab (Mabthera, Rituxan) has been shown to increase overall survival. Human IgG1 is thought to eliminate tumor cells via complement-dependent cytolysis (CDC) and antibody-dependent cellular cytotoxicity (ADCC), depending on the target, and also by direct pro-apoptotic signaling or growth factor receptor antagonism. Clynes *et al.* suggested that ADCC is a major *in vivo* mechanism of IgG1 action.[6] Recently, several mAb, including trastuzumab, which act predominantly via ADCC and CDC have been approved for the treatment of cancer patients. These include chimeric IgG1 mAb rituximab binding to the B-cell differentiation antigen CD20 for the treatment of B-cell lymphomas,[7] humanized IgG1 mAb trastuzumab targeting HER-2 overexpressed in a subgroup of breast cancers,[8] and humanized IgG1 alemtuzumab (Campath) targeting the differentiation antigen CD52 for the treatment of B-cell chronic lymphocytic leukemia.[9]

We hypothesized that ADCC is a possible mode of action of cetuximab against EGFR-expressing tumors. The present study was designed to clarify the role of cetuximab in ADCC and CDC activity, and to evaluate the relationship between EGFR expression status and cetuximab-mediated ADCC and CDC activity.

Methods

Cell lines and cultures. A human leukemia cell line (K562), a non-small cell lung cancer (NSCLC) cell line (A549) and a human embryonic kidney cell line (HEK293) were obtained from the American Type Culture Collection (Manassas, VA, USA). Human NSCLC cell lines A431, PC-9 and PC-14 were obtained from Tokyo Medical University (Tokyo, Japan). Human NSCLC cell lines Ma-1 and 11_18 were obtained from the National Cancer Center Research Institute (Tokyo, Japan). PC-9 and Ma-1 are known to contain E746_A750del, and 11_18 is known to contain L858R in tyrosine kinase domains of EGFR. The other cell lines are known to have wild-type EGFR. K562, HEK293, A431, PC-9, PC-14, Ma-1 and 11_18 cells were cultured in RPMI-1640 (Sigma, St Louis, MO, USA) supplemented with 10% heat-inactivated fetal bovine serum (FBS; Gibico BRL, Grand Island, NY, USA). A549 cells were cultured in Dulbecco's modified Eagle's medium (DMEM; Invitrogen, Carlsbad, CA) with 10% heat-inactivated FBS.

Plasmid construction and transfection. Construction of the mock expression plasmid vector (empty vector) and of the wild-type EGFR and 15-bp deletional EGFR (E746-A750del type deletion)

vectors, both of which possess the same deletion site as that observed in PC-9 cells, have been described elsewhere.[10] The plasmids were transfected into HEK293 cells and the transfectants were selected with Zeosin (Sigma). The stable transfectants (pooled cultures) of the empty vector, wild-type EGFR and its deletion mutant were designated 293M, 293W and 293D cells, respectively.

Compound. The mAb anti-EGFR cetuximab (IMC-225, Erbitux) was kindly provided by Bristol Myers Squibb (New York, NY, USA).

Analysis of EGFR expression on the cell surface. Cell surface expression of EGFR in tumor cell lines was quantified using a flow cytometric system (BD LSR; Becton-Dickinson, San Jose, CA, USA). The binding of cetuximab to tumor cell lines was titrated using FACS analysis. Cetuximab and another anti-EGFR mAb (R-1, sc-101; Santa Cruz Biotechnology, Santa Cruz, CA, USA) were used as the primary antibodies. Then, 1×10^6 tumor cells were incubated with 1 µg/mL cetuximab in 1% bovine serum albumin in phosphate-buffered saline (PBS) for 30 min at room temperature. After the first reactions, the cell surface was stained with 10 µg/mL fluorescein-conjugated antihuman IgG (Vector, Burlingame, CA, USA) for 45 min at room temperature in the dark. After the second reactions, the tumor cells were resuspended in 1 mL PBS. For analysis using the anti-EGFR mAb, 1 µg EGFR mAb per 1×10^6 tumor cells was used as the primary antibody. The secondary antibody was 10 µg/mL fluorescein-conjugated antimouse IgG (Vector). A minimum of 2×10^4 cells were analyzed by flow cytometry. Control experiments were carried out in the absence of primary antibodies. Data were analyzed with CellQuest software and the modifying program (Beckton Dickinson, CA, USA). The magnitude of surface expression of these proteins was indicated by the mean fluorescence intensity (MFI) of positively stained cells. The expression values were calculated as follows:

$$\text{Expression value} = (\text{MFI of positively stained cells})/(\text{MFI of control cells}).$$

The correlation between the expression of R-1-combined EGFR and that of cetuximab-combined EGFR were calculated using simple regression analysis.

Cytotoxicity assays. ADCC and CDC were examined using the CytoTox 96 Non-Radioactive Cytotoxicity Assay (Promega, Madison, WI). For quantification of ADCC activity, peripheral blood mononuclear cells were isolated from healthy volunteers with Lymphocyte Separation Medium (Cappel, Aurora, OH, USA) and used as effector cells. The target cells were suspended in RPMI medium without FBS and plated in a 96-well U-bottom microtiter plate at 5×10^3 cells/well. Cetuximab was added in triplicate to the individual wells at various concentrations from 0.001 to 10 µg/mL and effector cells were added at an effector : target cell ratio of 10:1. For quantification of CDC activity, human serum from a healthy volunteer was obtained as a compliment source. To yield a 1:3 final dilution, 50 µL serum was added. The plates were incubated for 4 h at 37°C, and the absorbance of the supernatants at 490 nm was recorded to determine the release of lactate dehydrogenase. The average of absorbance values for the culture medium background was subtracted from experimental release (A), target cell spontaneous release (B), effector cell spontaneous release (C) and target cell maximum release (D). The specific cytolysis percentage was calculated using the following formula:

$$\text{Cytotoxicity } (\%) = (A - B - C)/(D - B) \times 100.$$

The correlation between the expression of cetuximab-combined EGFR and ADCC activity was calculated using a simple regression analysis.

Growth-inhibition assay. We used the 3-(4,5-dimethylthiazol-2-y)-2,5-diphenyltetrazolium bromide (MTT) assay to evaluate the cytotoxicity of various drug concentrations. Two hundred microliters of an exponentially growing cell suspension was seeded in a 96-well microtiter plate, and cetuximab-containing solution was added at various concentrations (from 0.001 to 100 µg/mL). Each experiment was carried out in triplicate for each drug concentration and independently three times.

Growth inhibitory assay for the combination of gefitinib and cetuximab-mediated ADCC in the PC-9 cell line. We analyzed the growth inhibitory effect of the combination of gefitinib and cetuximab-mediated ADCC in the PC-9 cell line using the MTT assay. Two hundred microliters containing 1000 PC-9 cells, and various concentrations of gefitinib, were seeded in a 96-well microtiter plate. Then, 10 µL of cetuximab-containing solutions of various concentrations (from 0.1 to 10 µg/mL) and 20 000 effector cells were added.

Western blotting. PC-9, PC-14 and A549 cell lines were seeded in cell culture plates at a density of 6.0×10^5 cells/plate and allowed to grow overnight in appropriate maintenance cell culture media for each cell line containing 10% heat-inactivated FBS. The media were then replaced with RPMI-1640 (Sigma) (PC-9 and PC-14) or DMEM without FBS, with or without cetuximab (10 and 100 µg/mL). The cells were incubated for a further 24 h and stimulated or not stimulated with EGF (100 ng/mL) under serum starvation conditions. Cells were washed with ice-cold PBS and scraped immediately after adding 50 µL of M-PER mammalian protein extraction reagent (Pierce Biotechnology, Rockford, IL, USA). The protein extracts were separated by electrophoresis on 7.5% sodium dodecylsulfate–polyacrylamide gels and transferred to nitrocellulose membranes by electroblotting. The membranes were probed with a mouse monoclonal antibody against EGFR (Transduction Laboratory, San Diego, CA, USA), and phosphor-EGFR (specific for Tyr1068), Akt, phosphor-Akt, p44/42 MAPK and phosphor-p44/42 MAPK antibodies (Cell Signaling Technology, Beverly, MA, USA) as primary antibodies, followed by a horseradish peroxidase-conjugated secondary antibody. The bands were visualized with an electrochemiluminescence reagent (ECL; Amersham, Piscataway, NJ, USA).

Results

Binding properties of cetuximab to tumor cell lines expressing EGFR. The A431 cells expressed a high level of EGFR on their surfaces. Cell surface EGFR expression values of the PC-9, PC-14, A549, Ma-1 and 11_18 cell lines were lower than that of A431. The MFI for the K562 cells was less than 10 (Table 1). A good

Table 1. Epidermal growth factor receptor (EGFR) expression values and antibody-dependent cellular cytotoxicity (ADCC) activity

Cell liine	EGFR expression (R-1)	EGFR expression (cetuximab)	ADCC (%)
A431	286.2 ± 13.7	318.9 ± 98.2	30.7
PC-9	9.7 ± 6.2	20.1 ± 10.2	20.1
PC-14	17.6 ± 1.5	42.2 ± 8.6	26.8
A549	9.1 ± 1.9	19.1 ± 6.2	24.2
Ma-1	13.8 ± 1.4	27.5 ± 2.9	22.3
11_18	6.1 ± 0.6	12.6 ± 1.1	15.5
K562	1.1 ± 0.4	2.8 ± 1.6	7.0
293M	3.7 ± 1.6	8.6 ± 3.2	8.2
293W	40.19 ± 6.2	39.73 ± 6.2	16.3
293D	55.21 ± 21.9	53.04 ± 8.2	18.9

Expression values and ADCC activity were calculated as described in the Materials and Methods section. The mean of expression values from three different experiments and standard deviations are shown. The values for cetuximab-combined EGFR expression are shown for a concentration of 1 µg/mL.
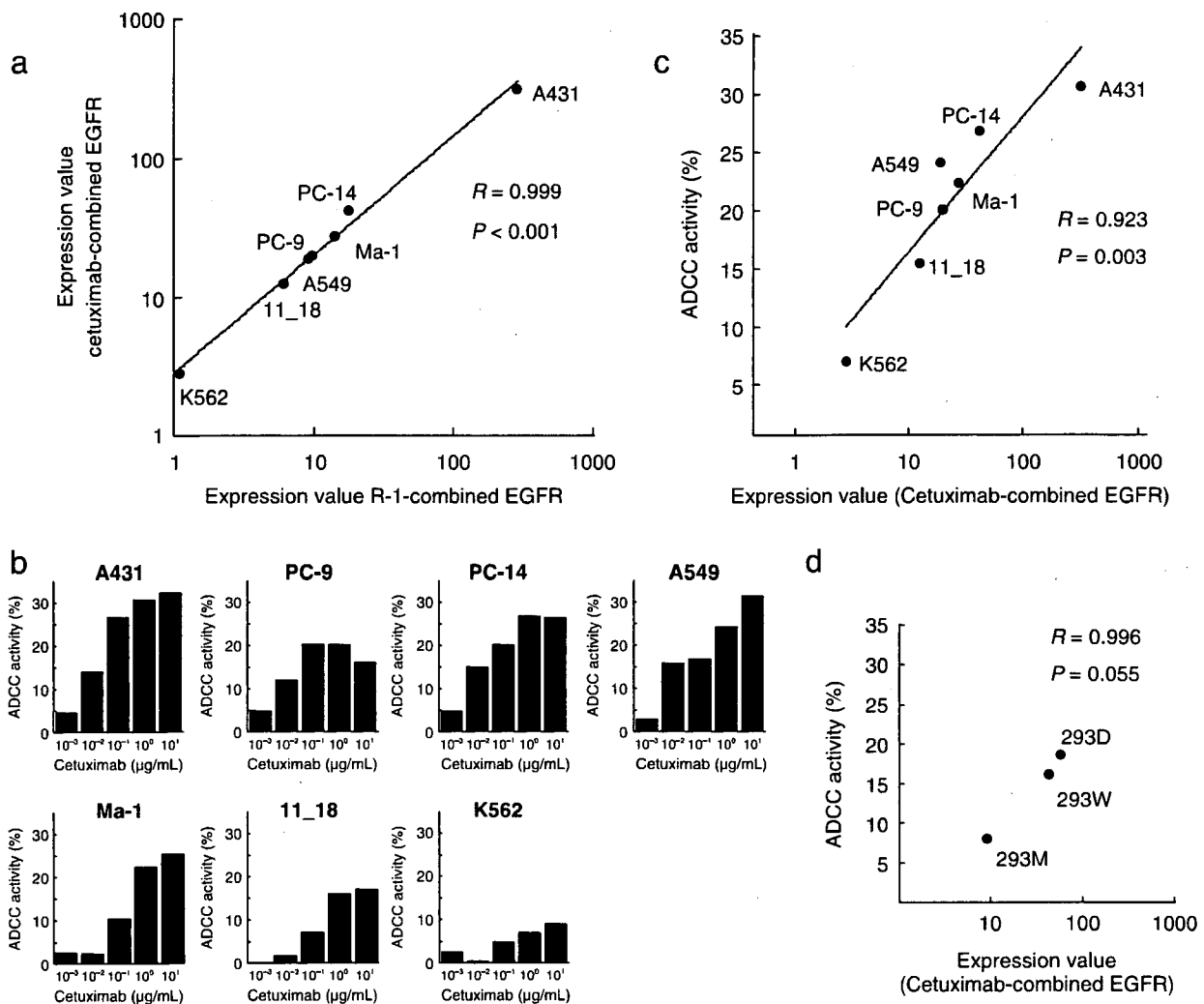
Fig. 1. Epidermal growth factor receptor (EGFR) expression and cetuximab-mediated antibody-dependent cellular cytotoxicity (ADCC) activity in the tumor cell lines. (a) Correlation between the expression of cetuximab-combined EGFR and R-1-combined EGFR. The values for cetuximab-combined EGFR expression are shown for a concentration of 1 μg/mL. The correlation coefficient between the results of these assays was 0.999. (b) Cetuximab-mediated ADCC activity in tumor cell lines at concentrations ranging from 0.001 to 10 μg/mL was determined using the CytoTox 96 Non-Radioactive Cytotoxicity Assay. (c) Correlation between expression values of cetuximab-combined EGFR and ADCC activity in the seven tumor cell lines. The values for cetuximab-combined EGFR expression and cetuximab-mediated ADCC activity are shown for a concentration of 1 μg/mL. The correlation coefficient between the results of these assays was 0.924. (d) Correlation between expression values of cetuximab-combined EGFR and ADCC activity in transfected HEK293 cell lines. The correlation coefficient between the results of these assays was 0.952.

correlation was observed between the binding of cetuximab and R-1 antibody with a correlation coefficient of 0.999 ($P < 0.001$; Fig. 1a).

ADCC and CDC activities in tumor cell lines. ADCC activities of cetuximab were detected in all tumor cell lines except K562 (Table 1; Fig. 1b). In the K562 cells, % ADCC activities were lower than 10% at all concentrations of cetuximab examined (from 0.001 to 10 μg/mL). ADCC activity mediated by cetuximab was highly correlated with the binding values of cetuximab to cells expressing EGFR ($R = 0.924$, $P = 0.003$; Fig. 1c). CDC activity was not detected in any of the cell lines in the cetuximab concentration range from 0.001 to 10 μg/mL.

Direct growth inhibitory effect of cetuximab on tumor cell lines. Cetuximab showed no growth inhibitory effect in any of the cell lines examined, regardless of EGFR expression levels. Even the highest concentration of cetuximab (100 μg/mL) did not inhibit growth in any of the cell lines (Fig. 2).

ADCC activities of cetuximab against the cells transfected with wild-type and mutant EGFR. EGFR expression was detected in 293W and 293D cells, but not in 293M cells (Table 1). The

ADCC activity mediated by cetuximab in 293W and 293D cells was dose dependent. In contrast, ADCC activities in 293M cells were <10% at all concentrations of cetuximab tested (0.001–10 μg/mL). There was a good correlation between the ADCC activities and the levels of cetuximab binding to EGFR in the cells ($R = 0.996$, $P = 0.055$; Fig. 1d). These results indicate that ADCC depends on the level of cetuximab binding to EGFR, but not the mutation status of the EGFR tyrosine kinase domains.

Direct growth inhibitory effect of the combination of gefitinib and cetuximab-mediated ADCC in the PC-9 cell line. The growth inhibitory effect in the PC-9 cell line was shown by effector cells at a gefitinib exposure exceeding 0.01 μM and was concentration dependent (Fig. 3). When cetuximab was added, growth was inhibited in a cetuximab concentration-dependent manner. An additive growth inhibitory effect was recognized between 0 and 0.01 μM of gefitinib. This additive growth inhibitory effect could not be evaluated at concentrations between 0.1 and 1.0 μM because of the strong inhibitory effect of gefitinib alone.

Effect of cetuximab on phosphorylation of EGFR and its downstream signaling molecules in NSCLC cells. Phosphorylation of EGFR
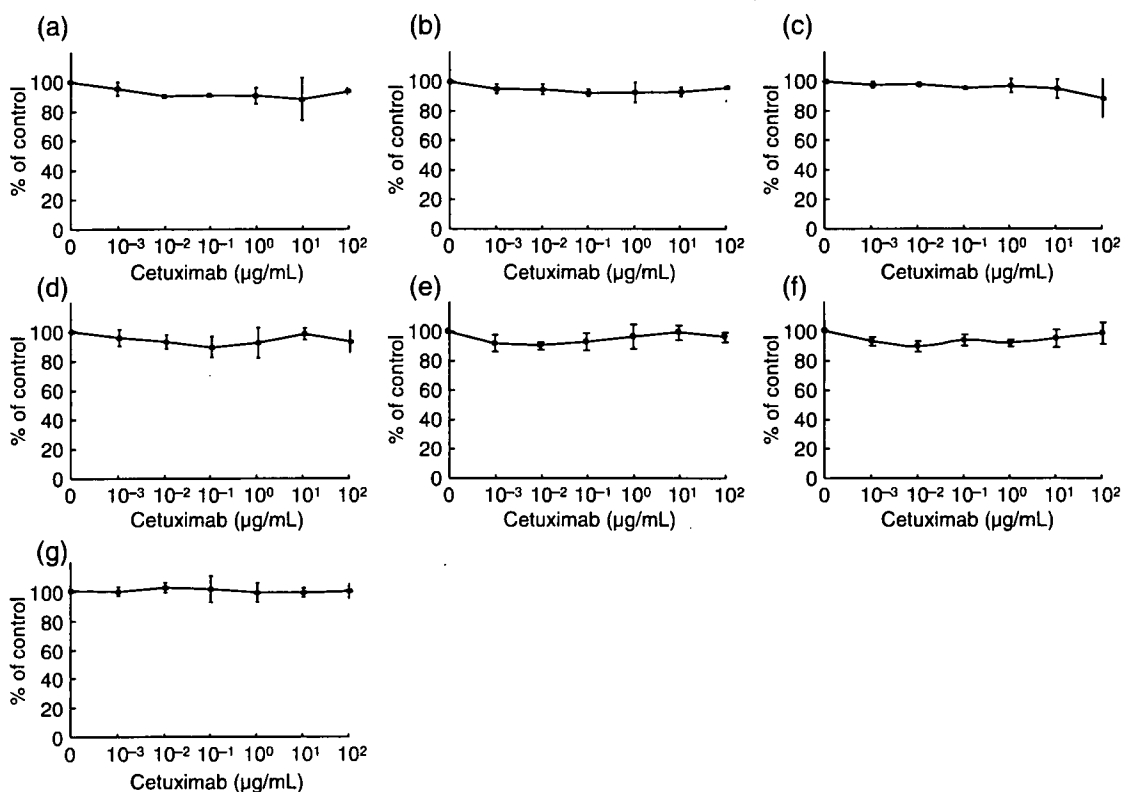
Fig. 2. Growth inhibitory effect of cetuximab on non-small cell lung cancer cell lines: (a) A431; (b) PC-9; (c) PC-14; (d) A549; (e) Ma-1; (f) 11_18; and (g) K562. Cell growth was not inhibited at any concentration, even a high concentration (10 μg/mL). The figure shows the dose-dependent growth inhibitory effect of gefitinib with various concentrations of cetuximab (0–10 μg/mL). Results are expressed as percentages of the untreated control value. The data shown are the mean + SD values from triplicate experiments.
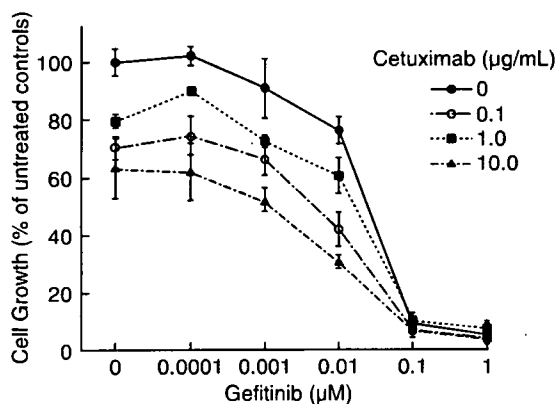

Fig. 3. Growth inhibitory effects of combining gefitinib and cetuximab-mediated antibody-dependent cellular cytotoxicity (ADCC). The figure shows dose-dependent growth inhibitory effects of gefitinib with various concentrations of cetuximab (solid circle, 0 μg/mL; solid square, 0.1 μg/mL; open circle, 1.0 μg/mL; solid triangle, 10 μg/mL). Results are expressed as a percentage of the untreated control value. The data shown represent the median values of triplicate experiments.

was strongly expressed in PC-9 regardless of EGF treatment, and the phosphorylation of EGFR continued the strong expression during cetuximab treatment. Phosphorylation of EGFR was slightly expressed in PC-14 and A549 without EGF treatment, but the phosphorylation of EGFR was enhanced by the EGF treatment. Although the enhancement of phosphorylation was inhibited dose dependently by cetuximab, the phosphorylation

was not completely inhibited at the highest concentration (10 μg/mL) of cetuximab. Phosphorylation of 44/42 MAPK and Akt was increased in all cell lines compared with the absence of EGF treatment. Although the increase in phosphorylation was diminished by adding cetuximab, phosphorylation was not completely inhibited at the highest concentration (10 μg/mL) of cetuximab (Fig. 4).

Discussion

Antibody therapies are a major approach in the treatment of various cancer types. Herein, we focused on the ADCC activity mediated by cetuximab against human lung cancer cells expressing wild-type or mutant EGFR. Neither CDC nor direct growth inhibition mediated by cetuximab was detectable in our experiments.

Direct growth inhibition, ADCC and CDC mediated by antibodies are the modes of action of antibody therapies. We previously demonstrated that ADCC is the major mode of action of trastuzumab in breast cancer cell lines, even when used in combination with cisplatin.[11] Cisplatin did not affect ADCC activity at the concentration for combined use in vitro. Clinical efficacies of cetuximab for various types of cancers have been demonstrated in many clinical studies using combinations with cytotoxic agents including cisplatin. Thus, ADCC is considered to be an important factor governing the efficacy of cetuximab.

Mukohara et al. reported that EGFR mutations in NSCLC cells are not associated with sensitivity to cetuximab in vitro.[12] They focused on the direct growth inhibitory effect of cetuximab against lung cancer cells. We previously demonstrated that PC-9 and 293 cells transfected with E746_A750del EGFR are
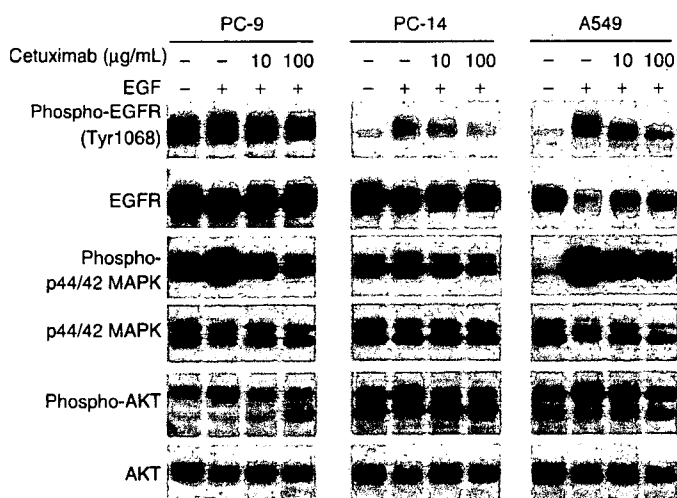
Fig. 4. Effects of cetuximab on phosphorylation of epidermal growth factor receptor (EGFR), Akt and p44/42 MAPK in non-small cell lung cancer cell lines. (a) EGFR mutant cell line PC-9 (with the E746_A750del mutation). (b) EGFR wild-type cell line PC-14. (c) EGFR wild-type cell line A549. Cells were treated with cetuximab at the indicated concentrations for 24 h. Immunoblots of cellular protein were analyzed for phosphorylated and total EGFR, p44/42 MAPK and Akt. The experiments were repeated at least twice.

hypersensitive to EGFR-tyrosine kinase inhibitors.[10] In contrast, we have demonstrated that ADCC activity mediated by cetuximab is not affected by EGFR mutation status in lung cancer cells or in 293 cells transfected with EGFR. Taken together, these observations indicate that cetuximab exerts its antitumor effects against human lung cancer cells independently of EGFR mutation status.

ADCC activity mediated by cetuximab has been demonstrated against 293 cells transfected with wild-type and mutated EGFR. Higher ADCC activity against 293D cells compared with 293W cells was observed ,with cetuximab exposure (Fig. 1d; Table 1). However, ADCC was correlated with EGFR expression levels in these transfectants. The activity appears to depend on expression levels but not mutation status.

Approximately 30 mutations of EGFR have been reported in lung cancer.[13-16] ADCC activity against PC-9 cells with E746_A750del in exon 19, one of the common mutations, has been demonstrated herein. We also examined ADCC activity against another human lung cancer cell line, 11_18,[17] with L858R in exon 21, which is another common mutation. Our results showed a strong positive correlation between ADCC activity and EGFR expression level, and that the impact on ADCC activity did not depend on the site of EGFR mutations.

Cetuximab is a chimeric antibody against the extracellular domain of EGFR. Other antitumor anti-EGFR antibodies currently under investigation clinically include humanized antibodies.[18] It remains unknown whether humanized and chimeric antibodies

exert ADCC activity against lung cancer differentially, and this awaits future investigation.

Some investigators have reported on the predictive factor and enhancement of ADCC activity mediated by certain mAb other than cetuximab.[19-22] Important ADCC-mediating effector cells that express receptors against the Fc region of IgG include monocytes and macrophages (FcγRI, IIa and IIb), granulocytes (FcgRII) and natural killer cells (FcγRIII).[19] One group of researchers demonstrated single nucleotide polymorphisms of FcγRIII in individual patients correlating with rituximab-dependent ADCC activity and the clinical response to rituximab.[20] Carson et al. demonstrated that the natural killer cell-mediated ADCC activity of breast cancer cell lines expressing HER2/neu, in the presence of trastuzumab, was markedly enhanced following stimulation with interleukin 2 and proposed the concurrent use of trastuzumab and interleukin-2 therapy in patients with cancers expressing HER2/neu.[21] However, from the view point of mAb but not effector cells, lack of fucosylation of the antibodies affects ADCC enhancement.[22] Whether or not these factors enhance cetuximab-mediated ADCC activity warrants further examination.

We showed additional growth inhibition by gefitinib and cetuximab in PC-9 cells. PC-9 cells had a deletional mutation in exon 19 of EGFR and hyper-responsiveness to gefitinib. We think that cetuximab-mediated ADCC increased the growth inhibition-independent response to gefitinib. The ADCC activity could not be evaluated at higher concentrations of gefitinib (>0.1 μM) because PC-9 cells were sufficiently inhibited at the higher concentrations. Additionally, we showed that some phosphorylations downstream of EGFR in NSCLC cell lines were mediated by cetuximab, although cetuximab had no growth inhibitory effect on the cell lines. We think that cetuximab-combined EGFR inhibits binding of EGFR and its ligands, such as EGF, and that phosphorylation downstream of EGFR is inhibited as a consequence of the addition of cetuximab. We have shown that phosphorylation of 44/42 MAPK and Akt in NSCLC cell lines was increased by EGF treatment and decreased by then adding cetuximab. Phosphorylation of EGFR in PC-14 and A549 cells was decreased with the addition of cetuximab, as in the 44/42 MAPK and Akt cell lines. Phosphorylation of EGFR in PC-9 cells was strongly increased without ligands under serum starvation conditions and was not decreased by cetuximab. Phosphorylation that was independent of ligand binding to EGFR seem not to be controlled by cetuximab.

These results conclude that cetuximab has ADCC activity against tumor cells with EGFR expression, and ADCC activity depends on the degree of EGFR expression on tumor cell surfaces, additionally leading us to believe that cetuximab treatment has clinical activity in EGFR-expressing tumor cells via cetuximab-mediated ADCC.

Acknowledgments

References

1 Salomon DS, Brandt R, Ciardiello F, Normanno N. Epidermal growth factor-related peptides and their receptors in human malignancies. Crit Rev Oncol Hematol 1995; 19: 183–232.

2 Selvaggi G, Novello S, Torri V et al. Epidermal growth factor receptor overexpression correlates with a poor prognosis in completely resected non-small-cell lung cancer. Ann Oncol 2004; 15: 28–32.

3 Mendelsohn J. Epidermal growth factor receptor inhibition by a monoclonal antibody as anticancer therapy. Clin Cancer Res 1997; 3: 2703–7.

4 de Bono JS, Rowinsky EK. The ErbB receptor family: a therapeutic target for cancer. Trends Mol Med 2002; 8: S19–26.

5 Mendelson J. Blockade of receptors for growth factors: an anticancer therapy – the fourth annual Joseph H Burchenal American Association of

Cancer Research Clinical Research Award Lecture. Clin Cancer Res 2000; 6: 747–53.

6 Clynes RA, Towers TL, Presta LG, Ravetch JV. Inhibitory Fc receptors modulate in vivo cytoxicity against tumor targets. Nat Med 2000; 6: 443–6.

7 Grillo-Lopez AJ, White CA, Varns C et al. Overview of the clinical development of rituximab: first monoclonal antibody approved for the treatment of lymphoma. Semin Oncol 1999; 26: 66–73.

8 Vogel C, Cobleigh MA, Tripathy D et al. First-line, single-agent Herceptin (trastuzumab) in metastatic breast cancer: a preliminary report. Eur J Cancer 2001; 37: S25–9.

9 Hale G, Zhang MJ, Bunjes D et al. Improving the outcome of bone marrow transplantation by using CD52 monoclonal antibodies to prevent graft-versus-host disease and graft rejection. Blood 1998; 92: 4581–90.

10 Arao T, Fukumoto H, Takeda M, Tamura T, Saijo N, Nishio K. Small in-frame deletion in the epidermal growth factor receptor as a target for ZD6474. *Cancer Res* 2004; **64**: 9101–4.

11 Naruse I, Fukumoto H, Saijo N, Nishio K. Enhanced anti-tumor effect of trastuzumab in combination with cisplatin. *Jpn J Cancer Res* 2003; **93**: 574–81.

12 Mukohara T, Engelman JA, Hanna NH *et al.* Differential effects of gefitinib and cetuximab on non-small-cell lung cancers bearing epidermal growth factor receptor mutations. *J Natl Cancer Inst* 2005; **97**: 1185–94.

13 Lynch TJ, Bell DW, Sordella R *et al.* Activating mutations in the epidermal growth factor receptor underlying responsiveness of non-small-cell lung cancer to gefitinib. *N Engl J Med* 2004; **350**: 2129–39.

14 Paez JG, Janne PA, Lee JC *et al.* EGFR mutations in lung cancer: correlation with clinical response to gefitinib therapy. *Science* 2004; **304**: 1497–500.

15 Pao W, Miller V, Zakowski M *et al.* EGF receptor gene mutations are common in lung cancers from 'never smokers' and are associated with sensitivity of tumors to gefitinib and erlotinib. *Proc Natl Acad Sci USA* 2004; **101**: 13 306–11.

16 Shigematsu H, Lin L, Takahashi T *et al.* Clinical and biological features associated with epidermal growth factor receptor gene mutations in lung cancers. *J Natl Cancer Inst* 2005; **97**: 339–46.

17 Nagai Y, Miyazawa H, Tanaka T *et al.* Genetic heterogeneity of the epidermal growth factor receptor in non-small cell lung cancer cell lines revealed by a rapid and sensitive detection system, the peptide nucleic acid-locked nucleic acid PCR clamp. *Cancer Res* 2005; **65**: 7276–82.

18 Bianco R, Daniele G, Ciardiello F, Tortora G. Monoclonal antibodies targeting the epidermal growth factor receptor. *Curr Drug Targets* 2005; **6**: 275–87.

19 Graziano RF, Fanger MW. Fc gamma RI and Fc gamma RII on monocytes and granulocytes are cytotoxic trigger molecules for tumor cells. *J Immunol* 1987; **139**: 3536–41.

20 Dall'Ozzo S, Tartas S, Paintaud G *et al.* Rituximab-dependent cytotoxicity by natural killer cells: influence of FCGR3A polymorphism on the concentration–effect relationship. *Cancer Res* 2004; **64**: 4664–9.

21 Carson WE, Parihar R, Lindemann MJ *et al.* Interleukin-2 enhances the natural killer cell response to Herceptin-coated Her2/neu-positive breast cancer cells. *Eur J Immunol* 2001; **31**: 3016–25.

22 Shinkawa T, Nakamura K, Yamane N *et al.* The absence of fucose but not the presence of galactose or bisecting N-acetylglucosamine of human IgG1 complex-type oligosaccharides shows the critical role of enhancing antibody-dependent cellular cytotoxicity. *J Biol Chem* 2003; **278**: 3466–73.

Personalized Medicine and Proteomics: Lessons from Non-Small Cell Lung Cancer

György Marko-Varga,[†,‡] Atsushi Ogiwara,[†,§,∥] Toshihide Nishimura,[§,∥] Takeshi Kawamura,[§,∥]
Kiyonaga Fujii,[§,∥] Takao Kawakami,[§,∥] Yutaka Kyono,[∥] Hsiao-kun Tu,[∥] Hisae Anyoji,[∥]
Mitsuhiro Kanazawa,[∥] Shingo Akimoto,[∥] Takashi Hirano,[⊥] Masahiro Tsuboi,[⊥] Kazuto Nishio,[§]
Shuji Hada,[#] Haiyi Jiang,[×] Masahiro Fukuoka,[△] Kouichiro Nakata,[◆] Yutaka Nishiwaki,[+]
Hideo Kunito,[§] Ian S. Peers,[◇] Chris G. Harbron,[◇] Marie C. South,[⁓] Tim Higenbottam,[▽,£]
Fredrik Nyberg,[*,▽,✩] Shoji Kudoh,[ƒ] and Harubumi Kato[⊥]

*Respiratory Biological Sciences, AstraZeneca R&D Lund, SE-221 87 Lund, Sweden, Clinical Proteome Center,
Tokyo Medical University, Shinjuku Sumitomo Building 17F, 2-6-1 Nishishinjuku, Shinjuku, Tokyo 163-0217,
Japan, Medical ProteoScope Company, Limited, Shinjuku Sumitomo Building 17F, 2-6-1 Nishishinjuku,
Shinjuku, Tokyo 163-0217, Japan, Department of Surgery, Tokyo Medical University, 6-7-1 Nishishinjuku,
Shinjuku, Tokyo 160-0023, Japan, Clinical Division, Research & Development, AstraZeneca K.K., Umeda Sky
Building Tower East, 1-88, 1-chome, Ohyodo-naka, Kita-ku, Osaka 531-0076, Japan, Clinical Science
Department, Research & Development, AstraZeneca K.K., Umeda Sky Building Tower East, 1-88, 1-chome,
Ohyodo-naka, Kita-ku, Osaka 531-0076, Japan, Department of Medical Oncology, Kinki University School of
Medicine, 377-2,Ohno-higashi, Osakasayama-city 589-8511, Osaka, Japan, Department of Respiratory Diseases,
Toho University School of Medicine, 6-11-1, Omori-nishi, Ota-ku, Tokyo 143-8541, Japan, Dept. of Thoracic
Oncology, National Cancer Centre Hospital East, 6-5-1, Kashiwanoha, Kashiwa-city, Chiba 277-8577, Japan,
Statistical Sciences, AstraZeneca R&D Alderley Park, Cheshire, UK, Cancer & Infection Statistics, AstraZeneca
R&D Alderley Park, Cheshire, UK, Medicine & Science, AstraZeneca R&D Charnwood, Loughborough LE11 5RH,
Leicestershire, UK, Sheffield University, Sheffield, UK, Epidemiology, AstraZeneca R&D Mölndal, SE-431 83
Mölndal, Sweden, Institute of Environmental Medicine, Karolinska Institute, Box 210,
SE-171 77 Stockholm, Sweden, and 4th Department of Internal Medicine, Nippon Medical School,
1-1-5, Sendagi, Bunkyo-ku, Tokyo 113-8603, Japan*

Personalized medicine allows the selection of treatments best suited to an individual patient and disease phenotype. To implement personalized medicine, effective tests predictive of response to treatment or susceptibility to adverse events are needed, and to develop a personalized medicine test, both high quality samples and reliable data are required. We review key features of state-of-the-art proteomic profiling and introduce further analytic developments to build a proteomic toolkit for use in personalized medicine approaches. The combination of novel analytical approaches in proteomic data generation, alignment and comparison permit translation of identified biomarkers into practical assays. We further propose an expanded statistical analysis to understand the sources of variability between individuals in terms of both protein expression and clinical variables and utilize this understanding in a predictive test.

* To whom correspondence should be addressed. Epidemiology, Astra-Zeneca R&D Mölndal, SE-431 83 Mölndal, Sweden; Tel, +46 31 706 5203; Fax, +46 31 776 3828; E-mail, Fredrik.Nyberg@astrazeneca.com.
† György Marko-Varga and Atsushi Ogiwara made equal contributions to this manuscript.
† Respiratory Biological Sciences, AstraZeneca R&D Lund.
§ Clinical Proteome Center, Tokyo Medical University.
∥ Medical ProteoScope Co., Ltd.
⊥ Department of Surgery, Tokyo Medical University.
ƒ Clinical Division, Research & Development, AstraZeneca K.K.
× Clinical Science Department, Research & Development, AstraZeneca K.K.

△ Department of Medical Oncology, Kinki University School of Medicine.
◆ Department of Respiratory Diseases, Toho University School of Medicine.
+ Dept. of Thoracic Oncology, National Cancer Centre Hospital East.
◇ Statistical Sciences, AstraZeneca R&D Alderley Park.
⁓ Cancer & Infection Statistics, AstraZeneca R&D Alderley Park.
▽ Medicine & Science, AstraZeneca R&D Charnwood.
£ Medical School, Sheffield University.
✩ Epidemiology, AstraZeneca R&D Mölndal.
° Institute of Environmental Medicine, Karolinska Institute.
ƒ Fourth Department of Internal Medicine, Nippon Medical School.

Introduction

A personalized medicine approach uses appropriate bio-markers to select treatments best suited for an individual patient and disease phenotype. A multiple biomarker approach (e.g., proteomics) has the advantage over conventional single biomarkers of combining many different pieces of information. Here, we review the key features of state-of-the-art proteomic profiling and introduce recent analytic developments to build a proteomic toolkit for use in personalized medicine, and we describe how these may be applied in a viable method for exploiting predictive proteomic fingerprints in the clinic. The potential of our proteomics toolkit hopefully brings us one step closer to a practical personalized medicine.

Cancer therapy is moving toward individually selected treatments, chosen not only according to tumor cell type but also based on the patient's predicted responsiveness to different classes of therapy or susceptibility to therapeutic adverse events. This emerging personalized medicine approach draws on both genotype and phenotype information, including protein expression. To implement personalized medicine, we need to develop effective biomarker tests predictive of response to treatment or susceptibility to adverse events. The benefits of personalized medicine are exemplified by considering interstitial lung disease (ILD) among non-small cell lung cancer (NSCLC) patients, which is associated with various kinds of chemotherapy treatment. A personalized medicine approach, using a simple blood test to predict those NSCLC patients at risk of developing ILD, would clearly be of great value.

We review current thinking and present some novel developments in a number of areas that have to be integrated to develop and then practically apply such tests in a clinical setting:

• The large scale collection of reliable and high quality phenotypic and clinical data and blood samples.

• Protein analysis in blood.

• Data acquisition, handling, combining and analysis.

• Interpretation and utilization of results in a clinical setting.

Clinical Background

A Motivating Example: Gefitinib (IRESSA) Treatment of NSCLC. The concepts of proteomics-based personalized medicine discussed in this article are very generally applicable. A motivating example that we will refer to in order to illustrate the potential benefits of personalized medicine is ongoing work in attempting to develop a simple blood test to address the potential occurrence of ILD in seriously ill NSCLC patients, the target group for the NSCLC treatment gefitinib.

Gefitinib is a "small molecule" inhibitor of the enzyme tyrosine kinase of the epidermal growth factor receptor (EGFR) family, such as erbB1. It is an approved therapy for advanced NSCLC in many countries and offers important clinical benefits (tumor shrinkage and improvement in disease-related symptoms) for "end-stage" patients. The large phase III ISEL (IRESSA Survival Evaluation in Lung Cancer) trial demonstrated some improvement in survival with gefitinib which failed to reach statistical significance compared with placebo in the overall population and in patients with adenocarcinoma.[1] However, in preplanned subgroup analyses, a significant increase in survival was shown with gefitinib in patients of Asian ethnicity and in patients who had never smoked.[1]

Analysis of the biomarker data from a subset of patients in the ISEL study suggested that patients with pretreated advanced NSCLC who have tumors with a high EGFR gene copy number (detected by fluorescent in situ hybridization [FISH]) have a higher likelihood of increased survival when treated with gefitinib compared with placebo.[2] Increased HER2 gene copy number has also been seen in tumors from patients who are responsive to gefitinib.[3] Somatic-activating mutations of EGFR in tumor tissue have also been associated with increased gefitinib responsiveness in patients with NSCLC.[4-7] Such mutations are more commonly found in tumor samples from patients of Asian origin and non-smokers.[8]

Following the ISEL subgroup analyses, and the biomarker evidence, it has become important to clarify which patients are more suitable for treatment with gefitinib. Analyses for both somatic-activating mutations and gene copy number require tumor tissue, which is not always available from the time of diagnosis; therefore, a blood test may represent a more versatile option and be of great value to clinicians.

With respect to tolerability, the search for a blood test that might include both genetic and proteomic biomarkers to define patients at risk of adverse effects from a drug, for example interstitial lung disease with gefitinib, is a focus of research.

Interstitial Lung Disease as a Complication in NSCLC Patients. ILD is a disease that afflicts the parenchyma or alveolar region of the lungs.[9] The alveolar septa (the walls of the alveoli) become thickened with fibrotic tissue. Associated with drug use, it can present precipitously with acute diffuse alveolar damage (DAD). The lungs show so-called "ground glass" shadowing on chest radiology, and patients complain of severe breathlessness. There are no effective treatments but patients can be supported by oxygen supplementation, corticosteroid therapy, or assisted ventilation. The process of alveolar damage is however fatal in some patients. ILD is a co-morbidity in patients with NSCLC.[10-16] Both diseases are associated with cigarette smoking,[17-20] and ILD is also considered to be associated with various kinds of lung cancer chemotherapy.[21-26]

In the ISEL study of gefitinib in NSCLC mentioned above, ILD-type events occurred in 1% of both placebo and gefitinib-treated patients.[1] Most ILD-type events occurred in patients of Asian origin, where placebo and treated patients had similar prevalences of respectively 4% and 3%. The rate observed in the gefitinib-treated arm was in line with earlier safety data from Japan and a large gefitinib post-marketing surveillance study in Japan (3322 patients), where the reported rate of ILD-type events was 5.8%.[27]

A simple blood test to predict the potential occurrence of ILD in seriously ill NSCLC patients before initiating treatments would clearly be of great value. This article describes the personalized medicine approach, which could be used to provide such a test. Consequently, the proteomics objectives of the preliminary phase of the study we describe were to verify the protein expression alterations in blood plasma from case patients (who developed ILD) and control patients (without ILD) treated by gefitinib, using a liquid chromatography–mass spectrometry/mass spectrometry (LC–MS/MS) proteomics platform.

Data and Sample Collection

To develop a personalized medicine test, it is essential to have access to an adequately sized collection of high quality tissue samples on which to perform proteomics analysis, with corresponding reliable diagnostic and clinical data.
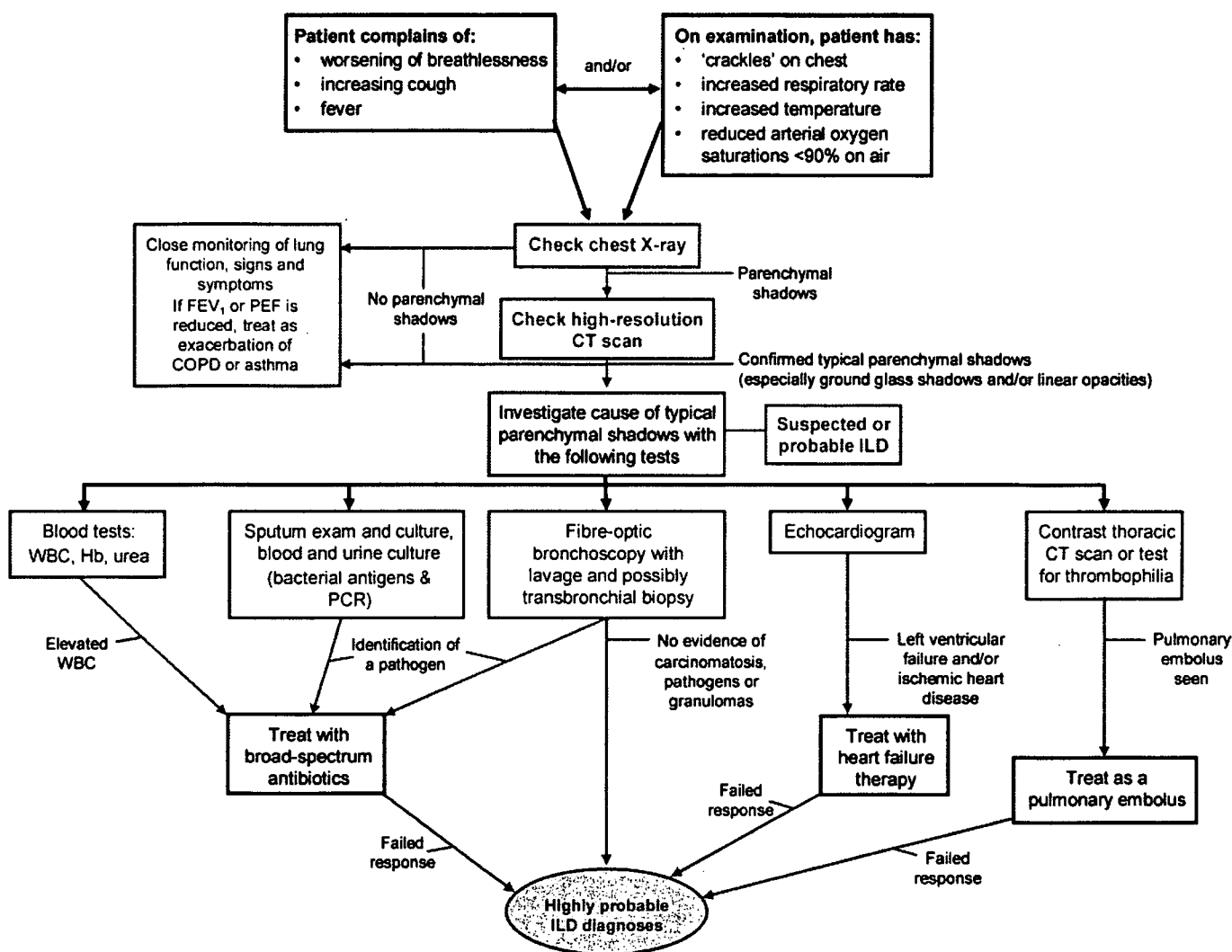
Figure 1. Algorithm for diagnosis of interstitial lung disease (ILD) in non-small cell lung cancer (NSCLC) patients.

As an example, in our work with gefitinib, samples were taken after obtaining informed consent from a nested case-control study, i.e., a case-control study performed within a prospective pharmacoepidemiological cohort of several thousand patients with advanced or recurring NSCLC who had received at least one prior chemotherapy regimen, and who were to be treated with gefitinib or chemotherapy. The main objective of this study was to measure the relative risk of ILD in Japanese patients with NSCLC using gefitinib compared with conventional therapy, with the associated aims of determining the incidence rate of ILD in late stage NSCLC patients and the principal risk factors for this complication.

Central to both the case-control study and the proteomics analysis was the use of internationally agreed criteria for the diagnosis of ILD and an algorithm of diagnostic tests to exclude alternative diseases.[28] Principal investigators in the study were asked to assess all patients for possible ILD using the diagnostic algorithm (Figure 1). Two case review boards of experts from oncology, radiology, and pulmonary medicine were set up to independently establish a consistent final diagnosis of ILD. In addition, extensive standard clinical and demographic risk factor data were collected on all registered cases and controls.

This degree of rigor in establishing accurate phenotypic diagnosis is critical to develop a robust and reliable personal-ized medicine test, as inaccuracies at this stage will affect all subsequent data analyses. The availability of clinical and risk factor data, and a rigorous epidemiological study design setting for the collection of proteomics samples is also of great value to fine-tune the statistical analysis.

Is Proteomics Ready for Personalized Medicine Applications?

The Human Proteome Map in Plasma. The impetus to develop personalized medicine based on blood samples has encouraged proteomic profiling that identifies individual proteins and multiple "fingerprint" protein patterns. A remaining limitation has been the lack of integration of the technology of protein separation with bioinformatics and statistical methods. Extensive national and international[29,30] collaborations are being implemented to address some of these needs. An important component in this development is the Human Proteome Organization (HUPO; www.HUPO.org), a scientific consortium that supports various programmes to map the proteins expressed in various human tissues, disease states, etc.[31–33] One of these is the Plasma Proteome initiative started in 2002, aiming to annotate and catalog the many thousands of proteins and peptides[34–37] of the human plasma proteome. Recently results from the pilot phase with 35 collaborating laboratories from 13 countries[38–42] and multiple analytical

groups were made publicly available on the Internet (www.bioinformatics.med.umich.edu/hupo/ppp; www.ebi.ac.uk/pride). The combined efforts have generated 15 710 different MS/MS datasets that were linked to the International Protein Index (IPI) protein IDs, and an integration algorithm applied to multiple matches of peptide sequences yielded 9504 IPI proteins identified with one or more peptides[40] and characterized by Gene Ontology, InterPro, Novartis Atlas, and OMIM. Such advances provide an important platform for transforming proteomics from a technology to a useful biomarker tool applicable to personalized medicine.

Protein Analysis in Blood—The Methods. With respect to automated studies, multidimensional chromatography is the main technology used for protein analysis in blood. It is coupled to mass spectrometry either by electrospray ionization (ESI) for analysis in solution or matrix assisted laser desorption/ionization (MALDI) in solid phase applications.[39,41,43-47] Alternatively, ion-trap mass spectrometers are gaining recognition for high-throughput sequencing.[46,48-53] Linking a Fourier transform ion cyclotrone resonance (FTICR) unit to the linear trap can increase the resolution profoundly,[36,54-56] one of several novel principles for strengthening the assignment of protein annotations with the most commonly used protein search engines.[36,47,54-61] For protein annotation, the recent development of a human protein reference database complements these technologies.[61] Studies of protein expression in a variety of biological compartments ranging from sub-cellular to whole organisms have been undertaken with these analytic approaches.[62-70] Some key findings from the HUPO initiatives that impact on methodology include:

- For studies using blood samples, plasma rather than serum is preferred, with ethylenediaminetetraacetic acid (EDTA) as an anticoagulant.[40]

- The abundant proteins in plasma should be depleted prior to analysis.[40]

- Acceptance of protein annotation, i.e., accepted protein identities[39,40] should use standard criteria. These include having two identified peptide sequences from each protein, both with a statistical significance score high enough to ensure a correct sequence confirmation when compared with the corresponding gene sequence entity.[39]

Despite the advances in methodology, important hurdles to using proteomics in a personalized medicine context remain.

Protein Expression Analysis in Blood—Some Important Hurdles. Although protein profiling technology is highly automated and interfaced with database search engines to relate peptide sequences to protein identities and function,[39,40] there are many practical reasons why determining the relative abundance of proteins relevant for prediction purposes is difficult:

- About 90% of proteins are believed to be present only in low copy numbers, i.e., at medium and low abundance levels.[49]

- There can be variation both in the quantity and form of protein expression within normal physiological function.

- Between 300 000 and 3 million human protein species exist as direct gene products or post-translational modifications.[44]

- The relative abundance of the post-translational modifications occurring within the cell is called a Cell-Protein-Index Number (CPIN).[29,30] As an example, if one considers that there are 30 types of phosphorylation variants of a single phosphoprotein, and a hundred possible fold forms of glycosylation of a single glycoprotein, the theoretical CPIN varies considerably depending on the sample complexity.

- The dynamic range of protein expression within cells, between levels of most and least abundant proteins, is in the order of 10^8–10^{10}.[34-36]

- In a typical clinical proteomics study the total cellular protein material in a sample seldom exceeds 10–20 milligrams. Therefore, the least abundant proteins would be present at starting levels not exceeding picograms.

- Recent studies use technology that can identify several thousand proteins in plasma samples,[29] but this still probably only represents a small fraction of the intermediate and processed protein forms. This is due to the current limitation of mass spectrometry not being able to ionize all amino acid sequences and protein modifications with equal efficiency. In most situations, a limited region of the full length protein is sequence annotated.

- The detection of differences in protein expression between groups of interest (e.g., cases and controls) takes place against a background of high variation between individuals within a group, within individuals over time and possible analytic run-to-run variation. Any method used to address this hurdle (which will involve "alignment" for spectral methods) directly impacts the ability to find good protein biomarkers.

Beyond the hurdles above, the fundamental challenge of protein biomarkers is to link the relative abundance of single markers or a fingerprint to clinically important biological processes based on some direct or indirect cause-effect link[29] related to normal or aberrant biological pathways.[47,49] In the following sections, we present the approach used for the identification of protein biomarkers potentially associated with development of ILD in NSCLC patients within the case-control study used as our motivating example. We build on the foundations described above and introduce further analytic developments and ideas relating to proteomic data generation, assaying and alignment to build a proteomics toolkit that can be applied today for personalized medicine approaches.

A State of the Art Clinical Biomarker Analysis System

In the previous section, we described several challenges in proteomic analysis. Here we describe a system and analysis approaches that we have successfully implemented to address some of these issues.

The Components of the Analysis System. The analysis system (Figure 2) uses liquid chromatography-based high-resolution separation of peptides with an interface to tandem MS/MS, a technology which has been attracting great attention as the "shotgun" method of proteome analysis.[44,68-70] With this technology, after depletion of albumin and immunoglobulin G (IgG), all extracted plasma proteins are digested into their specific peptide components by proteolytic enzyme treatment.

The generated peptides are subjected to capillary reverse-phase submicro- to micro-flow liquid chromatography (capillary RP μLC), separated by retention times due to their physicochemical properties, and then detected and sequenced by a linear ion-trap tandem mass spectrometer[71] (LTQ, Thermo Fisher Scientific, San Jose, CA) interfaced with a spray needle tip for ESI of peptides.[70] A two-dimensional quadrupole ion trap mass spectrometer[71] is used, operated in a data-dependent acquisition mode with operational m/z range limits set at 450–2000 (Figure 3, graphs A and B). Automatic switching to MS/MS acquisition mode is made in 1-second scanning cycles, controlled by the XCalibur software. The actual differences between annotated peptide fragment peaks shown in Figure 3, graph C, correspond to the amino acid residue mass, i.e.,
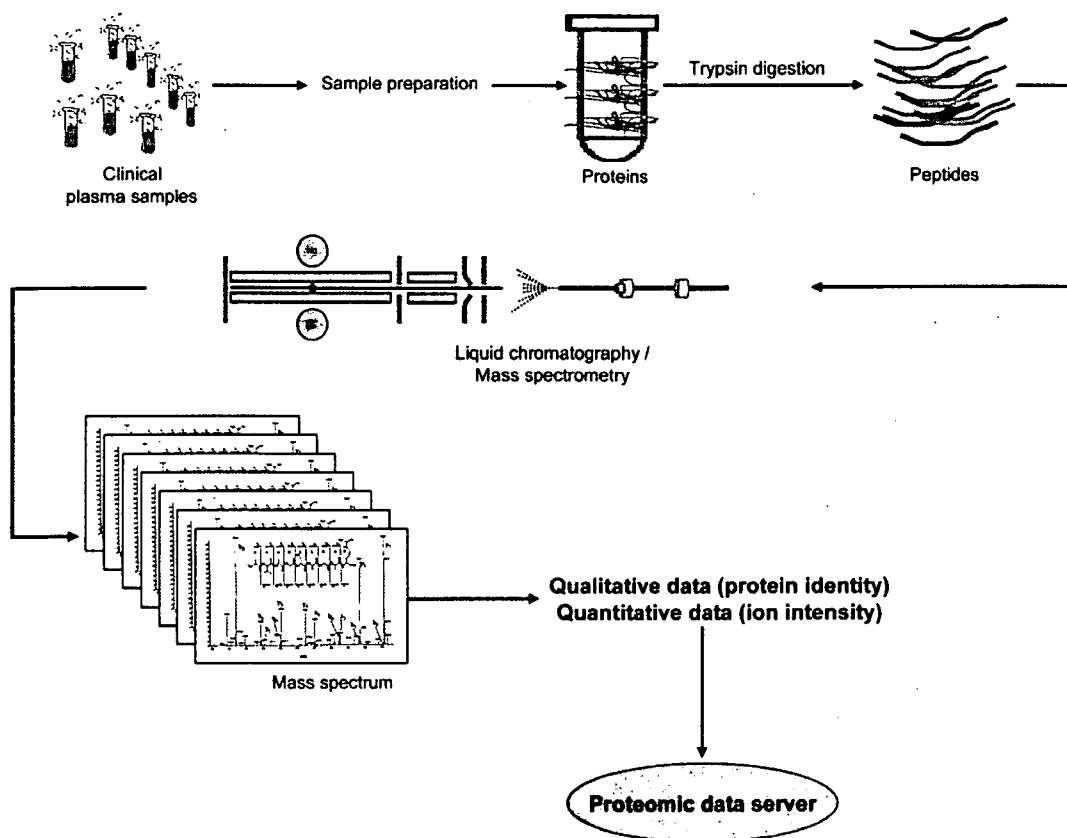
Clinical plasma samples → Sample preparation → Proteins → Trypsin digestion → Peptides

Liquid chromatography / Mass spectrometry

Mass spectrum

Qualitative data (protein identity)
Quantitative data (ion intensity)

Proteomic data server

Figure 2. Schematic illustration of the clinical proteomics screening process.

A) 3-D map of LC-MS data

Relative intensity

B) LC-MS Base peak profile

Relative intensity

Retention time, min.

C) A product ion spectrum from the precursor ion in the LC-MS data

Relative intensity

m/z
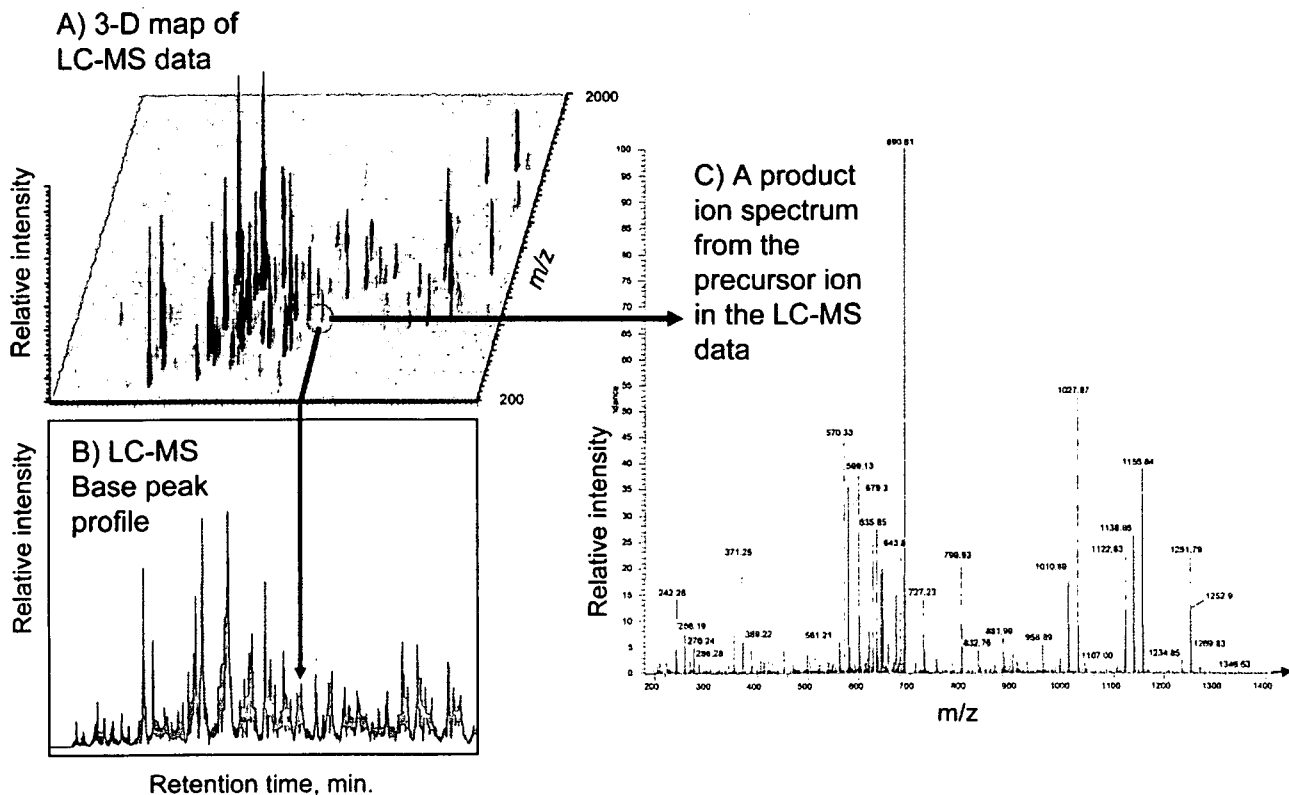
Figure 3. Profile of LC—MS data: (a) the three-dimensional view of LC-MS data, (b) the base-peak mass chromatogram, and (c) a product ion spectrum measured for a precursor ion in data-dependent acquisition mode (with MS acquisition operational *m/z* range set at 450—2000).
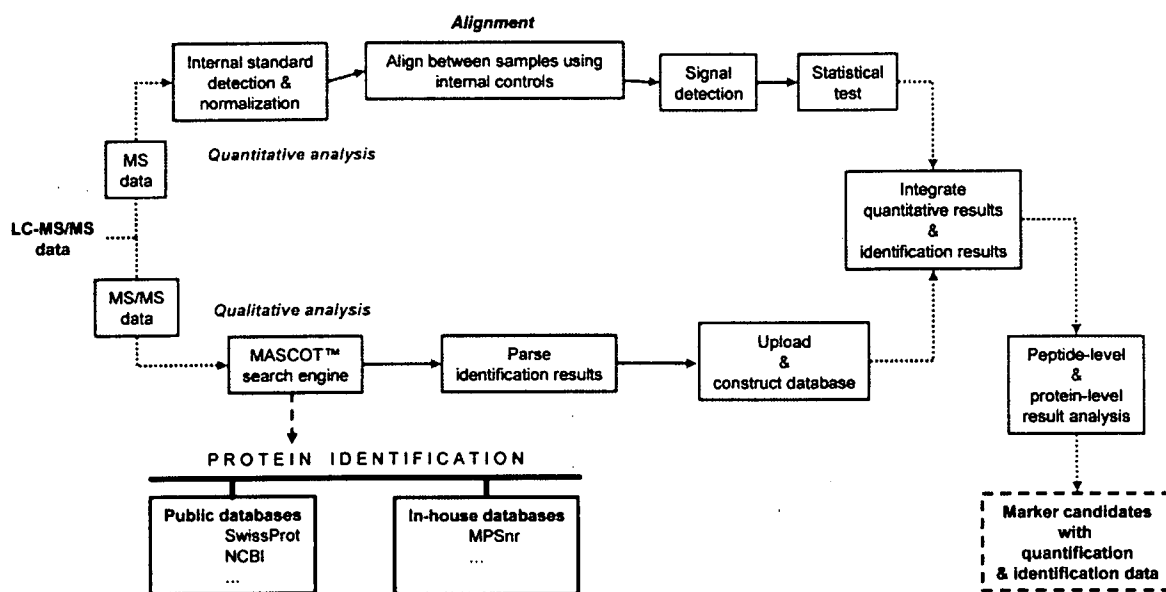
Figure 4. Overview of the data acquisition and database mining process developed within the gefitinib biomarker study.

identify the correct amino acid sequence. Internal standards are used for alignment of retention-times.

How the Methodology Overcomes Some of the Hurdles. The system described above addresses some of the hurdles noted previously. The digestion of all extracted plasma proteins into peptides will reduce the complexity by combining high-resolution nanoflow chromatographic fractionation with the separation power of modern mass spectrometry, performing automated and unattended shotgun sequencing in plasma.[35] Peptides are also more soluble and easier to handle than intact proteins. In addition, the two-dimensional quadrupole ion trap mass spectrometer[71] operates with a high-volume quadrupole electric field that makes it highly efficient to trap ions. The result is high sensitivity, high scanning speed, and better quantification over a wide dynamic range in comparison with the conventional three-dimensional ion-trap instruments.

Finding signals against a background of high variation is a further challenge, and the next section describes some approaches for addressing these.

Initial Data Handling, Processing, and Analysis

Proteomic data analysis process can be considered as consisting of two components (Figure 4). *Quantitative analysis* is used to discover significant differences in peptide signal intensities by comparing two (or more) sample groups. This process uses data collected from an entire MS run to quantify the amount of peptide ions by their respective ion signal intensity. *Qualitative analysis* is used to identify the amino acid sequence of each peptide ion, from the respective product ion spectra. To maximize their value, the results from the two component analyses should be considered in combination.

A typical quantitative analysis may consist of several steps:

1. Normalization: To account for differences in the original sample concentrations. Typically, the total signal intensity is scaled to a constant value for each analyzed sample.

2. Alignment: Correcting for nonlinear fluctuation in retention time between different samples. A variety of methodologies are available for aligning LC−MS data sets. We have found the i-OPAL algorithm (Patent # WO 2004/090526 AI), which is based on the single linkage clustering algorithm[72] and which makes

use of internal standard signals, to perform well. Other alignment algorithms include xcms.[73]

3. Peak picking or signal detection: Identifying individual peptide ions within the data.

4. Identify discriminating peptides: A number of methods can be used, often in combination. A common approach is to apply a Student's t-test and select peptides which are significant, i.e., with a p-value less than the chosen cutoff, and which also show a fold-change or intensity ratio greater than another criterion. Further developments of this aspect are discussed in the Principled Statistical Analysis section.

A popular choice for qualitative analysis is the MASCOT MS/MS ion search program.[74] This may be run against a number of different peptide sequence databases, for example the NCBI Nr, Refseq, Gene Ontology, HUGO, and Swiss-Prot sequence databases. The results of the quantitative analysis can then be combined with the qualitative analysis so that, for example, a peptide must be both discriminating and have annotation—i.e., have achieved a high MASCOT score showing confidence in identification—to be considered a candidate biomarker.

The approaches we have discussed above are focused on finding potentially discriminating proteins of clinical utility. In the following section, we describe the next stage in our thinking, namely how we could rapidly deploy in the clinic a viable method for exploiting a predictive proteomic fingerprint.

A Proposal for Proteomics in the Clinical Setting: Mass Spectrometric Biomarker Assays - MSBA

Although today's technology allows for high-throughput analyses of many proteins rather than a single protein,[30] the details of how such multiplexing assays will be adapted for clinical use have not been well clarified. The Mass Spectrometric Biomarker Assay (MSBA) platform described here was conceived as one example of a rapid and seamless method to progress from identification of a diagnostic more directly to a clinically useful test. MSBA requires only a minute sample amount (5−20 μL) to obtain a read-out from a handful of quantified protein biomarkers (typically 3−35) and automatically analyzes proteins using liquid-phase separation and tandem mass spectrometry with simultaneous quantitation and identification.
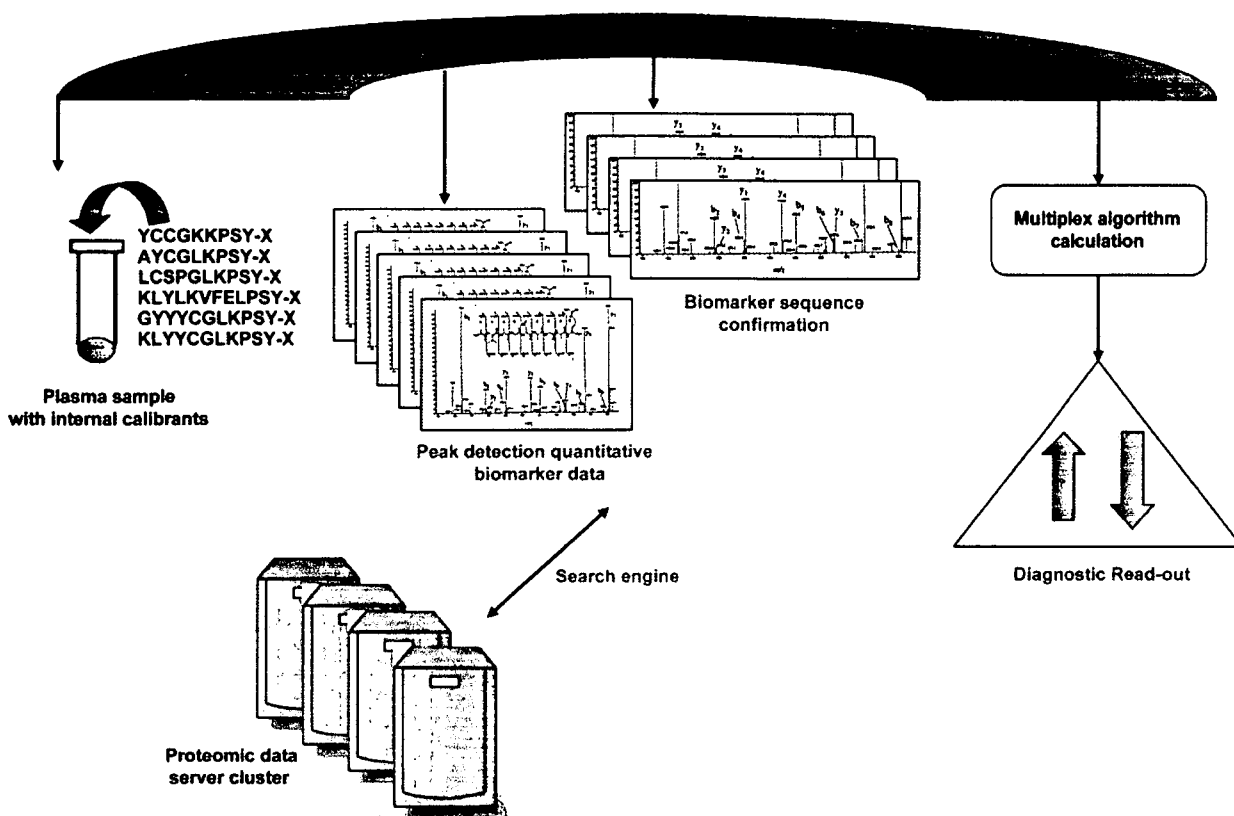
Figure 5. Entire flow of the operational components of Mass Spectrometric Biomarker Assays (MSBA).

The MSBA builds on a pre-defined Multiplex Biomarker list, which is stored within the MSBA database. Each marker entity has the values of masses and the relative retention time index with tolerance parameters. In running a patient sample, the predefined biomarker list is scanned to pick up patient sample signals that match with one of the predefined biomarker signals by satisfying the tolerance criteria (in general ± 1 for m/z value and $\pm 2\%$ for relative retention time index). The selected candidate signals are further confirmed using the product ion spectrum. That is, the product ion spectrum is represented as a vector by binning (grouping) the m/z ratio values. Using the cosine correlation between the sample vectors and the reference vectors, we can confirm whether the selected candidate signals are truly assigned as target biomarkers. (A standard threshold value of the cosine correlation is 0.8.)

The process steps within the MSBA cycle are outlined in Figure 5. The calculation of the final multiplex biomarker assay read-out from all of the individual markers can be performed by a variety of applications, as discussed in more detail in the Principled Statistical Modeling Approach section. Figures 6A and B illustrate one approach, calculating a distance score which indicates to what extent a measured sample is distant from the case or control template in terms of predefined multiplex biomarkers.

$$S_{\text{case or control}} = $$

$$\sqrt{\left[\frac{1}{n(n-2)}\right]\left[n\sum_i y_i^2 - \left(\sum_i y_i\right)^2 - \frac{\left[n\sum_i x_i y_i - \left(\sum_i x_i\right)\left(\sum_i y_i\right)\right]^2}{n\sum_i x_i^2 - \left(\sum_i x_i\right)^2}\right]}$$

If the ratio of S_{case} and S_{control} exceeds an MSBA threshold parameter, then the test sample is predicted to be a patient susceptible to develop ILD (ILD case); if not, the test sample is predicted to be a non-susceptible patient (control). We are currently evaluating the MSBA approach in practice.

A Principled Statistical Modeling Approach

We have described an analytical approach based on proteomic data, with various novel developments. However, additional insight is needed to further improve model discrimination and to broaden the focus from the proteomic data to the ultimate goal of prediction using combinations of data. Statistical analysis can be used to provide further refinement by combining information from the full clinical and laboratory datasets.

An advantage of a multiple biomarker approach (e.g., proteomics) compared with standard single biomarker development is the capability to combine information from many different entities. An example is illustrated in Figure 7A. Considering each biomarker alone fails to separate the two groups of subjects, as there is considerable overlap for both biomarkers. Use of two biomarkers in combination completely separates the two groups.

We can also use clinical variables to advantage in the analysis of the peptide patterns. For example, the efficacy of gefitinib appears to be greater in non-smokers, women, patients of Asian origin, and patients with adenocarcinomas.[8] Figure 7B illustrates how, instead of two protein biomarkers, the combination of clinical data (e.g., age) and a proteomic biomarker is able to separate two groups.

On this basis, we propose using a principled statistical analysis approach to first explore and understand the data and
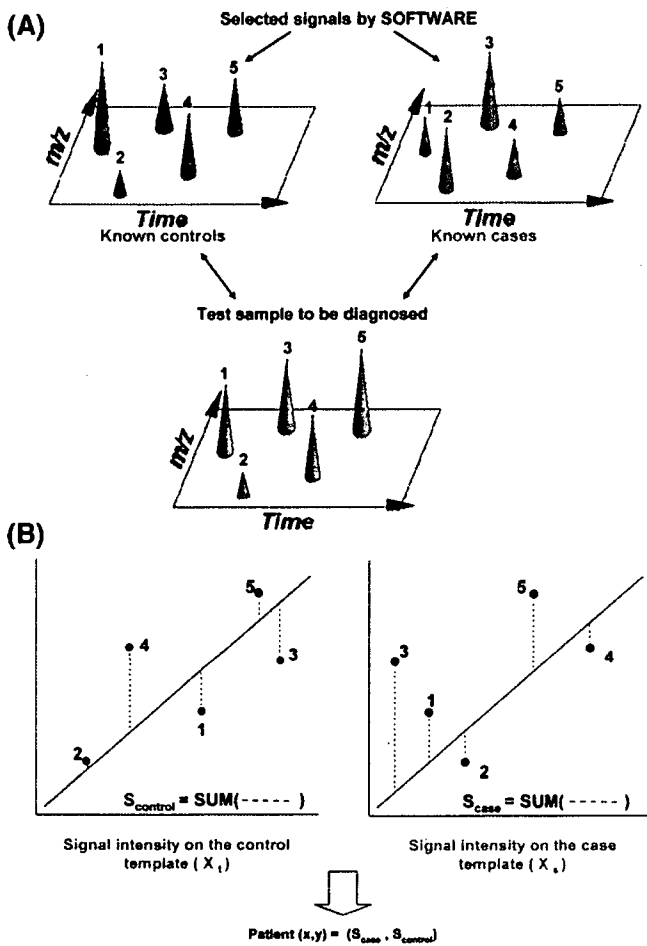
(A)

(B)

Figure 6. (A) Peptide signal comparison that MSBA (Mass Spectrometric Biomarker Assays) performs of the generated ions from the sample. The comparison is made both with the pattern of the controls and with the pattern of the case group for the corresponding signals. (B) Illustration of the regression model application of the MSBA where control templates and case templates are compared to that of the sample template generated in the analysis process.

then to model it and understand the quality of any models produced. A first step is to perform exploratory data analysis (EDA), for example using principal components analysis (PCA), to understand the major sources of data variation and the covariation between clinical parameters and protein intensity measures. The next step is univariate modeling for each protein marker individually, for example using analysis of covariance (ANCOVA), and an assessment of the effect of clinical parameters across the whole set of protein biomarkers using, for example, the False Discovery Rate as a tool.[75] This provides an understanding of key clinical variables and sources of variation within the data.

The next step is to perform multivariate predictive modeling using the proteins and clinical variables identified as being potentially important. There are a number of mathematical methods described in the literature for performing supervised classification, for example Support Vector Machines,[76] Random Forests,[77] PAM,[78] all of which have been successfully applied to high dimensional genomics data.[79] It remains an important unanswered question which modeling approach, or combination of modeling approaches, will generate the most predictive and robust models for data generated using this technology within a prospective study of this design.

Finally, to confirm that we have a practical prediction, the predictive power of a model must be assessed on a different set of patients from that used to generate the model. There are a number of approaches for external validation given a limited size dataset, for example the sequential approach of building a model based upon currently available data and testing on data from new patients when they become available, or withholding an arbitrary selection of subjects from the modeling as a test set and testing the model on these subjects. Internal validation approaches such as cross-validation or related bootstrapping methods may also be useful to assess the model selection *procedure*, but tend to overestimate the performance of a specific predictive model in subsequent external validation.[80,81] The key properties to consider when selecting an assessment method are to ensure that it will provide both precise and unbiased information regarding the prediction error rate of the potential model to be tested for clinical use. As well as assessing an overall predictive rate, it is also useful to separately assess the predictive rate for both the cases and controls and to consider the relative costs of making these false predictions within a clinical setting. Finally, the prevalence of the condition in question (here ILD) is also a critical factor in estimating what proportion of people predicted to be at risk are truly at risk, and this should also be borne in mind when evaluating a model for potential clinical use. The recently published FDA concept paper on drug-diagnostic co-
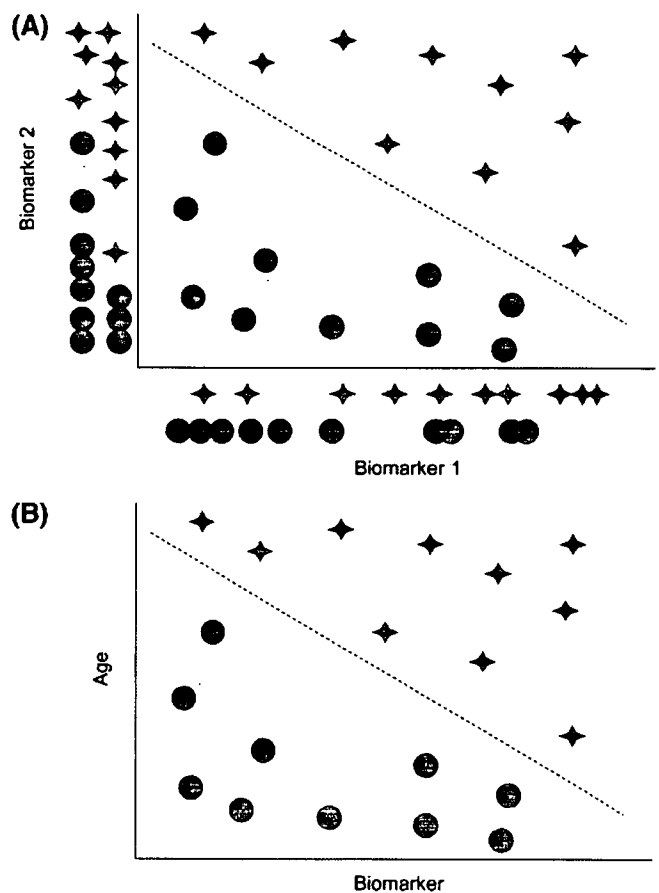
(A)

(B)

Figure 7. (A) Hypothetical example of the combined disease-linkage effect of two protein biomarkers. (Stars signify affected case individuals, circles non-affected control individuals). (B) Hypothetical example of the combined disease-linkage effect of a biomarker and a clinical variable. (Stars signify affected case individuals, circles non-affected control individuals).
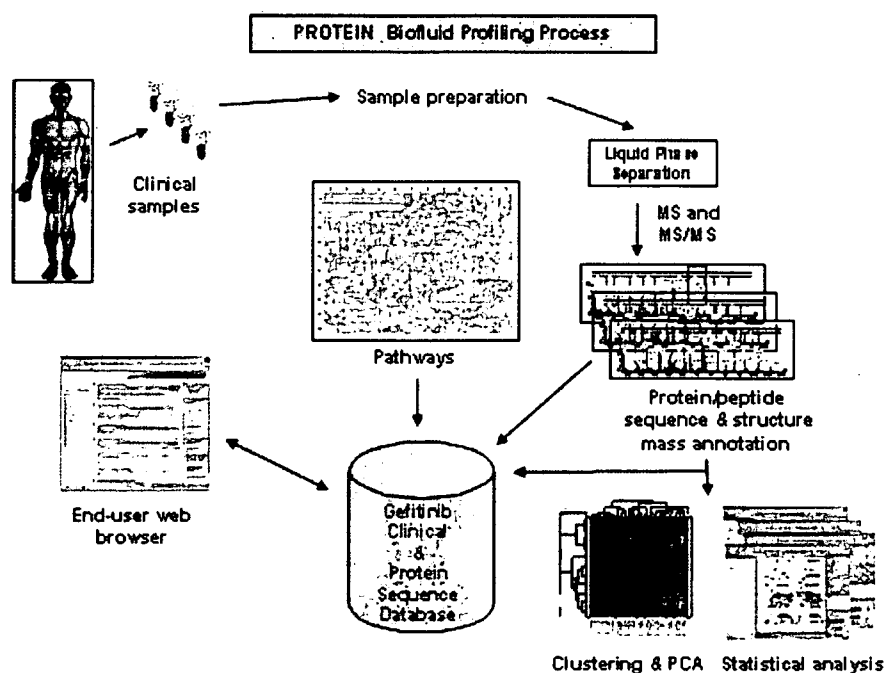
Figure 8. Illustration of the bioinformatics and data processing structure within which MSBA (Mass Spectrometric Biomarker Assays) data are captured, modified and analyzed.

development discusses many of the issues around validating predictive biomarkers.[82]

Finally, it is preferable to be able to assign a biological rationale to the biomarkers. Confidence in the reliability of a biomarker is greatly enhanced if we can correctly understand how it relates to the mechanism and progression of the disease of interest. Figure 8 illustrates a bioinformatics and data processing structure that we have developed to allow us to both conduct interactive exploratory and statistical analyses, and also investigate the disease and pathway linkage of discovered biomarker proteins through direct access to reference databases.

Future Perspectives

Within this paper we have discussed many of the issues that need to considered in developing a personalized medicine approach. A key starting point is that rigorous steps are taken to ensure accurate diagnosis and the careful gathering of both clinical and proteomic data to facilitate the search for peptide patterns.

There are many challenges in performing protein analysis in blood, but mass spectrometry equipment and methods can now be used to generate peptide data with high sensitivity, high scanning speed, and improved quantification. Data handling and processing techniques for steps such as peak alignment and the subsequent methodologies for statistical modeling and analysis are now far enough developed to generate high quality data and robustly analyze these data with confidence.

We have provided details of the MSBA method that can be used to easily translate protein intensities into a practical multiplex assay which can be exploited in the clinic without the need to develop anti-bodies for ELISA. We have also described how an expanded statistical analysis can be used to allow for the individual variance of protein expression to enable us to focus on the proteomic patterns that are actually related to ILD. Finally, we have emphasized the importance of validat-

ing the predictive power of a biomarker tool in a way that reflects the real-life setting of intended clinical use.

Hopefully, this combination of developments over a range of different areas brings us one step closer to a practical personalized medicine.

IRESSA is a trademark of the AstraZeneca group of companies.

References

(1) Thatcher, N.; Chang, A.; Parikh, P.; Pereira, J. R.; Ciuleanu, T.; von Pawel, J.; et al. Gefitinib plus best supportive care in previously treated patients with refractory advanced non-small-cell lung cancer: results from a randomised, placebo-controlled, multicentre study (Iressa Survival Evaluation in Lung Cancer). *Lancet* **2005**, *366*, 1527−1537.
(2) Hirsch, F. R.; Varella-Garcia, M.; McCoy, J.; West, H.; Xavier, A. C.; Gumerlock, P.; et al. Increased epidermal growth factor receptor gene copy number detected by fluorescence in situ hybridization associates with increased sensitivity to gefitinib in patients with bronchioloalveolar carcinoma subtypes: a Southwest Oncology Group study. *J. Clin. Oncol.* **2005**, *23*, 6838−6845.

(3) Cappuzzo, F.; Varella-Garcia, M.; Shigematsu, H.; Domenichini, I.; Bartolini, S.; Ceresoli, G. L.; et al. Increased HER2 gene copy number is associated with response to gefitinib therapy in epidermal growth factor receptor-positive non-small-cell lung cancer patients. *J. Clin. Oncol.* **2005**, *23*, 5007–5018.

(4) Araki, J.; Okamoto, I.; Suto, R.; Ichikawa, Y.; Sasaki, J. Efficacy of the tyrosine kinase inhibitor gefitinib in a patient with metastatic small cell lung cancer. *Lung Cancer* **2005**, *48*, 141–144.

(5) Kim, K. S.; Jeong, J. Y.; Kim, Y. C.; Na, K. J.; Kim, Y. H.; Ahn, S. J.; et al. Predictors of the response to gefitinib in refractory non-small cell lung cancer. *Clin. Cancer Res.* **2005**, *11*, 2244–2251.

(6) Lynch, T. J.; Bell, D. W.; Sordella, R.; Gurubhagavatula, S.; Okimoto, R. A.; Brannigan, B. W.; et al. Activating mutations in the epidermal growth factor receptor underlying responsiveness of non-small-cell lung cancer to gefitinib. *N. Engl. J. Med.* **2004**, *350*, 2129–2139.

(7) Paez, J. G.; Jänne, P. A.; Lee, J. C.; Tracy, S.; Greulich, H.; Gabriel, S.; et al. EGFR mutations in lung cancer: correlation with clinical response to gefitinib therapy. *Science* **2004**, *304*, 1497–1500.

(8) Shigematsu, H.; Lin, L.; Takahashi, T.; Nomura, M.; Suzuki, M.; Wistuba II; et al. Clinical and biological features associated with epidermal growth factor receptor gene mutations in lung cancers. *J. Natl. Cancer Inst.* **2005**, *97*, 339–346.

(9) American Thoracic Society: American Thoracic Society/European Respiratory Society International Multidisciplinary Consensus Classification of the Idiopathic Interstitial Pneumonias. This joint statement of the American Thoracic Society (ATS), and the European Respiratory Society (ERS) was adopted by the ATS Board of Directors, June 2001 and by The ERS Executive Committee, June 2001. *Am. J. Respir. Crit. Care Med.* **2002**, *165*, 277–304.

(10) Raghu, G.; Nyberg, F.; Morgan, G. The epidemiology of interstitial lung disease and its association with lung cancer. *Br. J. Cancer* **2004**, *91* (Suppl. 2), S3–S10.

(11) Asada, K.; Mukai, J.; Ougushi, F. Characteristics and management of lung cancer in patients with idiopathic pneumonia. *Jap. J. Thor. Dis.* **1992**, *51*, 214–219.

(12) Hubbard, R.; Venn, A.; Lewis, S.; Britton, J. Lung cancer and cryptogenic fibrosing alveolitis. A population-based cohort study. *Am. J. Respir. Crit. Care Med.* **2000**, *161*, 5–8.

(13) Matsushita, H.; Tanaka, S.; Saiki, Y.; Hara, M.; Nakata, K.; Tanimura, S.; et al. Lung cancer associated with usual interstitial pneumonia. *Pathol. Int.* **1995**, *45*, 925–932.

(14) Ogura, T.; Kondo, A.; Sato, A.; Ando, M.; Tamura, M. Incidence and clinical features of lung cancer in patients with idiopathic interstitial pneumonia. *Nihon Kyobu Shikkan Gakkai Zasshi* **1997**, *35*, 294–299.

(15) Takeuchi, E.; Yamaguchi, T.; Mori, M.; Tanaka, S.; Nakagawa, M.; Yokota, S.; et al. Characteristics and management of patients with lung cancer and idiopathic interstitial pneumonia. *Nihon Kyobu Shikkan Gakkai Zasshi* **1996**, *34*, 653–658.

(16) Turner-Warwick, M.; Lebowitz, M.; Burrows, B.; Johnson, A. Cryptogenic fibrosing alveolitis and lung cancer. *Thorax* **1980**, *35*, 496–499.

(17) Baumgartner, K. B.; Samet, J. M.; Stidley, C. A.; Colby, T. V.; Waldron, J. A. Cigarette smoking: a risk factor for idiopathic pulmonary fibrosis. *Am. J. Respir. Crit. Care Med.* **1997**, *155*, 242–248.

(18) Britton, J.; Hubbard, R. Recent advances in the aetiology of cryptogenic fibrosing alveolitis. *Histopathology* **2000**, *37*, 387–392.

(19) Iwai, K.; Mori, T.; Yamada, N.; Yamaguchi, M.; Hosoda, Y. Idiopathic pulmonary fibrosis. Epidemiologic approaches to occupational exposure. *Am. J. Respir. Crit. Care Med.* **1994**, *150*, 670–675.

(20) Nagai, S.; Hoshino, Y.; Hayashi, M.; Ito, I. Smoking-related interstitial lung diseases. *Curr. Opin. Pulm. Med.* **2000**, *6*, 415–419.

(21) Lilly. Gemcitabine prescribing information. http://pi.lilly.com/gemzar.pdf, 2003.

(22) Kunitoh, H.; Watanabe, K.; Onoshi, T.; Furuse, K.; Niitani, H.; Taguchi, T. Phase II trial of docetaxel in previously untreated advanced non-small-cell lung cancer: a Japanese cooperative study. *J. Clin. Oncol.* **1996**, *14*, 1649–1655.

(23) Merad, M.; Le Cesne, A.; Baldeyrou, P.; Mesurolle, B.; Le Chevalier, T. Docetaxel and interstitial pulmonary injury. *Ann. Oncol.* **1997**, *8*, 191–194.

(24) Wang, G.-S.; Yan, K.-Y.; Perng, R.-P. Life-threatening hypersensitivity pneumonitis induced by docetaxel (taxotere). *Br. J. Cancer* **2001**, *85*, 1247–1250.

(25) Erasmus, J. J.; McAdams, H. P.; Rossi, S. E. Drug-induced lung injury. *Semin. Roentgenol.* **2002**, *37*, 72–81.

(26) Aviram, G.; Yu, E.; Tai, P.; Lefcoe, M. S. Computed tomography to assess pulmonary injury associated with concurrent chemoradiotherapy for inoperable non-small cell lung cancer. *Can. Assoc. Radiol. J.* **2001**, *52*, 385–391.

(27) Yoshida, S. The results of gefitinib prospective investigation. *Med. Drug J.* **2005**, *41*, 772–789.

(28) Mueller, N. L.; White, D. A.; Jiang, H.; Gemma, A. Diagnosis and management of drug-associated interstitial lung disease. *Br. J. Cancer* **2004**, *91*, S24–S30.

(29) Marko-Varga, G.; Fehniger, T. E. Proteomics and disease—the challenges for technology and discovery. *J. Proteome Res.* **2004**, *3*, 167–178.

(30) Marko-Varga, G.; Lindberg, H.; Lofdahl, C. G.; Jonsson, P. H. L.; Dahlback, M.; Lindquist, E.; et al. Discovery of biomarker candidates within disease by protein profiling: principles and concepts. *J. Proteome Res.* **2005**, *4*, 1200–1212.

(31) Omenn, G. S. The Human Proteome Organization Plasma Proteome Project pilot phase: reference specimens, technology platform comparisons, and standardized data submissions and analyses. *Proteomics* **2004**, *4*, 1235–1240.

(32) Omenn, G. S. Advancement of biomarker discovery and validation through the HUPO plasma proteome project. *Dis. Markers* **2004**, *20*, 131–134.

(33) Orchard, S.; Hermjakob, H.; Binz, P. A.; Hoogland, C.; Taylor, C. F.; Zhu, W.; et al. Further steps towards data standardisation: the Proteomic Standards Initiative HUPO 3(rd) annual congress, Beijing 25–27(th) October, 2004. *Proteomics* **2005**, *5*, 337–339.

(34) Anderson, N. G.; Matheson, A.; Anderson, N. L. Back to the future: the human protein index (HPI) and the agenda for postproteomic biology. *Proteomics* **2001**, *1*, 3–12.

(35) Anderson, N. L.; Anderson, N. G. The human plasma proteome: history, character, and diagnostic prospects. *Mol. Cell. Proteomics* **2002**, *1*, 845–867.

(36) Jacobs, J. M.; Adkins, J. N.; Qian, W. J.; Liu, T.; Shen, Y.; Camp, D. G.; et al. Utilizing human blood plasma for proteomic biomarker discovery. *J. Proteome Res.* **2005**, *4*, 1073–1085.

(37) Anderson, N. G.; Anderson, L. The Human Protein Index. *Clin. Chem.* **1982**, *28*, 739–748.

(38) Haab, B. B.; Geierstanger, B. H.; Michailidis, G.; Vitzthum, F.; Forrester, S.; Okon, R.; et al. Immunoassay and antibody microarray analysis of the HUPO Plasma Proteome Project reference specimens: systematic variation between sample types and calibration of mass spectrometry data. *Proteomics* **2005**, *5*, 3278–3291.

(39) Martens, L.; Hermjakob, H.; Jones, P.; Adamski, M.; Taylor, C.; States, D.; et al. PRIDE: the proteomics identifications database. *Proteomics* **2005**, *5*, 3537–3545.

(40) Omenn, G. S.; States, D. J.; Adamski, M.; Blackwell, T. W.; Menon, R.; Hermjakob, H.; et al. Overview of the HUPO Plasma Proteome Project: results from the pilot phase with 35 collaborating laboratories and multiple analytical groups, generating a core dataset of 3020 proteins and a publicly-available database. *Proteomics* **2005**, *5*, 3226–3245.

(41) Patterson, S. D. Data analysis—the Achilles heel of proteomics. *Nat. Biotechnol.* **2003**, *21*, 221–222.

(42) Rahbar, A. M.; Fenselau, C. Integration of Jacobson's pellicle method into proteomic strategies for plasma membrane proteins. *J. Proteome Res.* **2004**, *3*, 1267–1277.

(43) Ho, Y.; Gruhler, A.; Heilbut, A.; Bader, G. D.; Moore, L.; Adams, S. L.; et al. Systematic identification of protein complexes in Saccharomyces cerevisiae by mass spectrometry. *Nature* **2002**, *415*, 180–183.

(44) Aebersold, R.; Mann, M. Mass spectrometry-based proteomics. *Nature* **2003**, *422*, 198–207.

(45) Anderson, N. L.; Polanski, M.; Pieper, R.; Gatlin, T.; Tirumalai, R. S.; Conrads, T. P.; et al. The human plasma proteome: a nonredundant list developed by combination of four separate sources. *Mol. Cell. Proteomics* **2004**, *3*, 311–326.

(46) Olsen, J. V.; Mann, M. Improved peptide identification in proteomics by two consecutive stages of mass spectrometric fragmentation. *Proc. Natl. Acad. Sci. U.S.A.* **2004**, *101*, 13417–13422.

(47) Sadygov, R. G.; Liu, H.; Yates, J. R. Statistical models for protein validation using tandem mass spectral data and protein amino acid sequence databases. *Anal. Chem.* **2004**, *76*, 1664–1671.

(48) Fujii, K.; Nakano, T.; Kanazawa, M.; Akimoto, S.; Hirano, T.; Kato, H.; et al. Clinical-scale high-throughput human plasma proteome analysis: lung adenocarcinoma. *Proteomics* **2005**, *5*, 1150–1159.